Master Thesis

Development of a DP system for CS Enterprise I with Voith Schneider thrusters.

NTNU – Trondheim
Norwegian University of
Science and Technology

Håkon Nødset Skåtun

Department of Marine Technology — NTNU 2011

NTNU Trondheim
Norwegian University of Science and Technology
Department of Marine Technology

MASTER THESIS IN MARINE CYBERNETICS

Name of the candidate: Håkon Skåtun

Field of study: Marine control engineering

Thesis title (Norwegian): Utvikle eit DP system for CS Enterprise I med Voith Schneider thrustere.

Thesis title (English): Development of a DP system for CS Enterprise I with Voith Schneider thrusters.

Background

An offshore supply model ship, named CS Enterprise I (CS stands for CyberShip), has been procured in relationship with the Marine HIL Simulation Lab and MC Lab, for use by students in control engineering projects and demonstrations. The model ship has been equipped with two Voith Schneider main propellers aft and a tunnel thruster fore.

In this master thesis the aim is to perform mechanical completion, hardware-in-the-loop (HIL) simulation, and "sea trials" of the ship when controlled by:

- remote manual thruster control,
- remote joystick control, and
- automatic dynamic positioning,

incl. appropriate human-machine interfaces (HMIs) in the MC Lab.

This work includes mechanical outfitting, instrumentation of necessary electronics, development of mathematical models for HIL testing and model-based control designs, development of a HIL test setup and a basin test setup, system identification of model parameters, and experimental testing.

The candidate shall mainly target modeling, design, and implementation for a DP operation mode. Tentatively, the candidate may also consider a seakeeping mode of operation. Model parameters should be estimated based on experimental data series for the corresponding models, both by force measurement tests when rigged to the towing carriage and by free-floating tests. The Matlab System Identification Toolbox should be used for calculation of the model parameters based on the tests.

Work description

1. Carry out the mechanical outfitting and instrumentation of the model ship. Emphasis should be placed on how to control the Voith Schneider propellers and the tunnel thruster in order to generate the desired thrust vectors.
2. Develop a detailed mathematical model of the CSE1 with Voith Schneider propellers for slow-speed motion in calm water. A discussion on the Voith Schneider propellers is expected.
3. Develop a remote manual thruster command function for CSE1, incl. applicable HMI functions based on LabView, for individual control of each propeller.
4. Develop a thrust allocation algorithm for DP, mapping desired generalized forces (within allowed configuration space) to individual setpoints for the three propellers.
5. Perform system identification and model validation of the mathematical models by experimental testing in MC Lab.
6. Discuss the dynamic properties of the ship w.r.t. speed, bollard pull, maneuverability, and efficiency of the Voith Schneider propellers.
7. Develop a remote joystick command function, incl. applicable HMI functions based on LabView, for commanding the generalized propulsion forces on the ship.
8. Develop an automatic stationkeeping mode, incl. applicable HMI functions based on LabView, for the ship.

All control modes (manual, joystick, and DP) shall be thoroughly tested by HIL simulation before experimental testing is performed in the MC Lab basin.

Guidelines
The scope of work may prove to be larger than initially anticipated. By the approval from the supervisor, described topics may be deleted or reduced in extent without consequences with regard to grading.

The candidate shall present his personal contribution to the resolution of problems within the scope of work. Theories and conclusions should be based on mathematical derivations and logic reasoning identifying the various steps in the deduction.

The report shall be organized in a rational manner to give a clear exposition of results, assessments, and conclusions. The text should be brief and to the point, with a clear language. The report shall be written in English (preferably US) and contain the following elements: Abstract, acknowledgements, table of contents, main body, conclusions with recommendations for further work, list of symbols and acronyms, references and (optional) appendices. All figures, tables, and equations shall be numerated. The original contribution of the candidate and material taken from other sources shall be clearly identified. Work from other sources shall be properly acknowledged using a Harvard citation style (e.g. *natbib* Latex package). Any plagiarism is taken very seriously by the university, and any such practice will have consequences. NTNU can use the results freely in its research work, unless otherwise agreed upon, by properly referring to the work.

The thesis shall be submitted in 3 printed copies, each signed by the candidate. The final revised version of this project description must be included. The report must appear in a bound volume or a binder according to the NTNU standard template. Computer code and a PDF version of the report should be included electronically.

A 15 min. presentation (conference style) should be given on your main results at time around delivery.

Start date: 1 February, 2011 **Due date:** As specified by the administration.

Supervisor: Professor Roger Skjetne
Co-advisor(s): Ph.d. stud. cand. Øivind K. Kjerstad

Trondheim,

_____

Roger Skjetne
Supervisor

Summary

A model ship named CS Enterprise 1 (CSE1) has been purchased by the Norwegian University of Science and Technology (NTNU) to be used for demonstrations and student experiments at the Marine Cybernetics Laboratory (MC Lab). This model ship has in this project been equipped with two Voith Schneider Propellers (VSPs), and a new bow thruster, in addition instrumentation for these new actuators have been installed. Once the outfitting was completed, the aim was to develop a manual thruster control, joystick mode control, and a Dynamic Positioning (DP) system. In order to develop a DP system a system identification of the vessel was needed. This was performed by a combination of measurements and analysis from free-running tests using Matlabs System Identification ToolBox (SITB).

CSE1 were equipped with VSPs, a new bow thruster, and instrumented in the MC Lab. A manual thruster control was developed, where a PlayStation 3 (PS3) controller was used for user input, allowing the operator to control all the vessels actuators precisely and simultaneously. For the system identification, the linear surge and sway damping were found by towing the model ship at different speeds, and measuring the drag forces with force sensors. Force sensors were also used to measure the thrust from the VSPs and the bow thruster at different set-points. Then-free-running tests were conducted, where the position and orientation of the vessel as well as the thruster set-points were recorded. This data was then fitted to a simplified DP model, using Matlabs SITB. The results from these analyzes were rejected as the standard deviation for the results were to high, and the method failed to provide consistent results. The vessel parameters from another model ship about the same size and geometry were therefore adopted to form the basis of the tuning of the DP controller. A proper Human Machine Interface (HMI) where created in LabView to monitor and control the vessel for all operational modes. This HMI includes a 3D window that displays the position and orientation of the model ship in real time. A Hardware In the Loop (HIL) simulator has also been implemented in order to test the DP controller, and verify signal routing and saturations.

With the performed upgrades and instrumentation of CSE1 the vessel should be well suited for demonstrations and student experiments. The use of the PS3 controller provided a great way to control the model boat. The method of using SITB for system identification partially failed because the simplified DP model was used, and this model

does not include some of the dynamics of the input data used. A more sophisticated model should be used as a grey-box model as this might improve the reliability of the estimated parameters. After some tuning of the DP controller and thrust allocation a working DP system were demonstrated, even though the DP system had some performance issues.

Preface

The work presented in this report is my master thesis written at NTNU during the spring 2011. This concludes my five years at the University.

During my work with this thesis, I have gained knowledge on a wide range of topics. I have got to work with subjects that I in advance had knowledge about, as well as subjects that were completely new to me. This might reflect my interest in how things are tied together, and my belief in that great solutions to problems are created when one combines different fields of science. Working with this thesis has been very motivating, and it has given me a lot in return, both theoretically, and on a personal experience level. To be able to combine both theory and practice have been really exciting, and I am very grateful to have had this privilege.

I would like to express my gratitude to my supervisor, professor Roger Skjetne, for his encouragement, guidance, and support, and for granting me the privilege of getting to use the University's lab facilities. I would also like to thank my co-advisor Ph.D stud. cand. Øivind Kåre Kjerstad, who has provided me with his expertise and moral support, and for all the help with the mechanical retrofit of CS Enterprise 1. Staff Engineer Torgeir Wahl at MARINTEK/Sintef has really helped me out with all the practical aspects related to the MC Lab, and I would really like to tank him for all his support, all his patience, and for introducing me to the world of electrical engineering. Last, but not least I would like to thank my girlfriend Lone for all her love and support, and for joining me at laboratory during the Easter holiday to comply with the SHE regulations, allowing me to work during the holiday.

I hope that other will find inspiration in my work, and that subsequent users of the model ship CS Enterprise 1 will benefit from my work effort and findings.

Trondheim, June 13, 2011

_____

Håkon Nødset Skåtun

Contents

List of Figures

List of Tables

List of Acronyms

AC Alternating Current

AHTS Anchor Handling Tug Supply

CRP Contra-Rotating Propellers

CS2 CyberShip 2

CSE1 CS Enterprise 1

DAQ Data AQquisition

DC Direct Current

DOF Degrees Of Freedom

DP Dynamic Positioning

ESC Electronic Speed Control

FPGA Field-programmable gate array

FPSO Floating Production, Storage and Offloading

GUI Graphical User Interface

HIL Hardware In the Loop

HIL Lab Hardware In the Loop Laboratory

HMI Human Machine Interface

HW hardware

IR Infra Red

JONSWAP Joint North Sea Wave Project

LF Low Frequency

LQG Linear Quadratic Gaussian

MC Lab Marine Cybernetics Laboratory

MIMO Multiple Input Multiple Output

NI National Instruments

NTNU Norwegian University of Science and Technology

PID Proportional, Integral, and Derivative

PS3 PlayStation 3

PSV Platform Supply Vessel

PWM Pulse Width Modulation

QTM Qualisys Track Manager

SHE Safety, Health, and Environment

SIT Simulation Interface Toolkit

SITB System Identification ToolBox

SNAME Society of Naval Architects and Marine Engineers

SW software

USB Universal Serial Bus

VSP Voith Schneider Propeller

WF Wave Frequency

List of Symbols

Chapter 1

Introduction

"Det sies at veien blir til mens man går
men det er vanskelig å forestille seg at båten blir til mens man ror..."

"It is said that the road becomes when walking,
but it's hard to imagine that the boat becomes while you row..."

-Anders Endahl

1.1 Motivation

DP systems have grown more and more complex over the years, and is today installed on almost all ships within the oil industry. The oil exploration in the North Sea would in many cases be extremely expensive, or not to say impossible without DP systems. Model testing provides a great way to try out new ship concepts, as well as new types of control systems. Gaining better knowledge about ships dynamics and the behavior of control systems is important to continuously improve safety and performance. Throughout this thesis a model ship will be built, and these initial modifications will provide a basic framework for others that later will come and do experiments and research with this model ship.

1.2 Background

In 2009, NTNU purchased a hobby model boat kit named Azis [Model Slipway, 2011]. The model boat kit was built by a professional model boat builder, fully configured to

build specifications with machinery, radio remote control communication, and painting. The purpose of this purchase was to have a new model ship to be used by MSc students and PhD students studying marine cybernetics at NTNU. In addition, the model ship should be suitable to be used for other kinds of demonstrations, such as recruitment demonstration, where the aim is to recruit young people to start a career in the discipline of marine technology. The model boat Azis was going to be a part of the newly founded Hardware In the Loop Laboratory (HIL Lab). The HIL Lab was founded by professor Roger Skjetne, and its purpose is to provide marine cybernetics students at NTNU with the necessary hardware (HW), software (SW) and other tools to do research and experiments on the topic of HIL. The HIL Lab is operated in close relations with the MC Lab.

The ship models used at the MC Lab have a long history of being named "CyberShip". However, due to the fact that professor Roger Skjetne is a great fan of the TV series "Star Treck", "Azis" was renamed to "CS Enterprise 1", after the star cruiser "Starship Enterprise 1" from the TV series. In our case *CS* stands for *CyberShip*.

Even though CSE1 was delivered "ready to run", the model ship needed major modifications to fulfill the requirements to be used as a testing and experimental platform. It was suggested earlier that CSE1 should be equipped with VSPs and have its bow thruster upgraded. In addition a Data AQquisition (DAQ) needed to be installed in the model ship. The DAQ's main function is to read sensor inputs from the model ship, and provide control signals for the actuators.

The scope for this thesis is to perform the actual upgrades on CSE1, such that the vessel can be used for experiments, and eventually create a DP system. These initial upgrades will also serve as a basic framework for others that later will use CSE1 for tests and experiments.

The final goal of this thesis after the mechanical outfitting of CSE1 is completed, is to design and implement a simple DP system for the model ship.

1.3 Dynamic Positioning

The International Maritime Organization [1994] gives the following definition of a DP vessel:

> "*Dynamically positioned vessel (DP-vessel) means a unit or a vessel which automatically maintains its position (fixed position or predetermined track) exclusively by means of thruster force.*"

and defines a DP system as:

> "*Dynamic positioning system (DP-system) means the complete installation necessary for dynamic positioning a vessel comprising of the following sub-systems*":
>
> - *power system*
> - *thruster system, and*
> - *DP-control system*

The idea of a system that would automatically position a ship only using its thrusters originated in the oil industry in the United States in the 1960s. The oil companies were drilling for oil on continuously increasing water depths, and soon it became obvious that the traditional way of using anchors to maintain a drilling rigs position was not feasibly any more. This paved the road for the evolution of DP systems. The first DP systems were relatively simple systems with analog controllers that had little or no redundancy. The world's first vessel to be equipped with what we today consider a DP was the "Eureka", which used a taut wire system for position reference. It did not take long before other types of vessels such as diver support vessels, cable laying vessels, survey vessels and so on started to be equipped with DP systems. By the late 1970's, DP had become a well established technique, and in 1980 the number of DP vessels was 65, and in 1985 the number has passed 150 vessels [Bray, 2003].

In Norway, professor Jens Glad Balchen started to collaborate with *Kongsberg Våpenfabrikk* in the early 1970s. Balchen believed that the DP systems of his time could be significantly improved. Already in 1977, *Kongsberg Våpenfabrikk* delivered its first DP system named Albatross to the ship "Seaway Eagle". Over the years *Kongsberg Våpenfabrikk* has turned into *Kongsberg Maritime* and are the world's leading supplier of DP systems. In 1999 Norwegian engineers voted the Albatross Positioning System the "second most important engineering feat of the century" in a competition hosted by *"Teknisk Ukeblad"* [Ryvik, 2011]. The Norwegian "oil adventure" would have been difficult to achieve without the DP technology.

Today DP systems can be found on a wide range of different vessel types, for instance Anchor Handling Tug Supply (AHTS) vessels, crane vessels, heavy lift vessels, Floating Production, Storage and Offloading (FPSO) vessels, militarily vessels and luxury yachts. Today DP systems are considered as an important safety feature.

When at sea, a vessel is exposed for different environmental loads, such as wind, waves, and current. These loads will result in a drift of a vessel. The main objective of the DP system is to counteract these environmental loads by using the ships propulsors such that the ship maintains its desired position and heading. This is illustrated in Figure 1.1 on the following page.

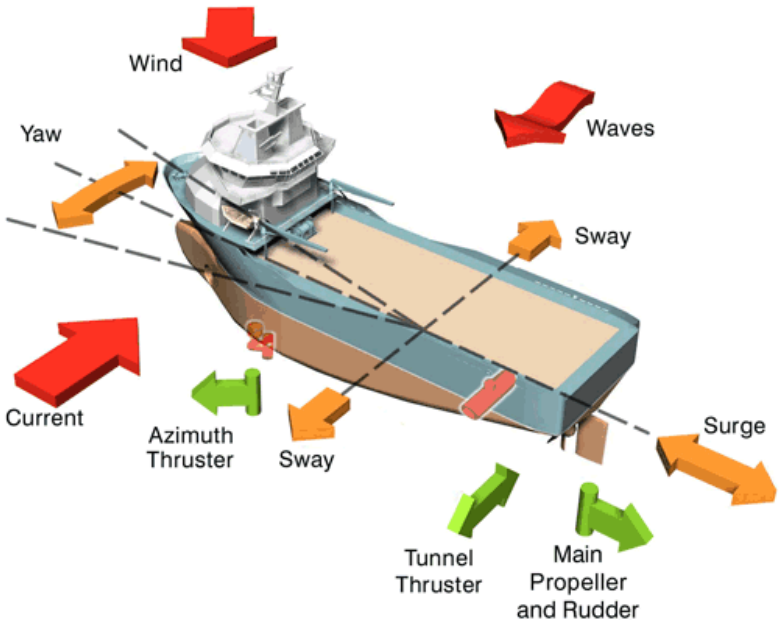

Figure 1.1: Dynamic positioning system - Basic forces and motions. [Courtesy: Kongsberg Maritime, 2011]

1.4 Hardware In the Loop

During the years marine control systems have grown more and more complex, and testing and verification of such control systems are important. HIL testing provides a great way to test the software on a marine control system. A HIL simulator operates in real time in closed-loop with the control computer system hardware and software and facilitates realistic and efficient testing of the control system functionality, performance, and failure handling functions [Skjetne and Egeland, 2006]. A definition of a HIL simulator is given by Skjetne and Egeland [2006]

HIL simulator: A real-time simulator, constructed by hardware and software, that is configured for the control system under consideration, embedded in external hardware, and interfaced to the target system or component through appropriate I/O. During execution the target system or component will not experience any qualitative difference from being integrated to the real system.

1.5 Scope

This thesis is divided into two parts. Where the first part describes the building process and upgrades of CSE1, and the infrastructure of the vessel and its surroundings. The second part reports the making of a DP system for CSE1

- Chapter 2 describes the building process of CSE1 in details.
- Chapter 3 presents the MC Lab, its features and how the tools, hardware, and systems are connected to CSE1.
- Chapter 4 describes the VSP and its basic working principles.
- Chapter 5 describes how a manual thruster control was made for CSE1.
- Chapter 6 explains the mathematical models used for the DP control system.
- Chapter 7 presents the different methods used to perform a system identification of CSE1.
- Chapter 8 guides the reader through the design process of the controllers, and HMI for the DP system.
- Chapter 9 presents results from HIL simulations and experiments.
- Chapter 10 discusses the thesis and gives recommendations.
- Chapter 11 concludes the thesis.

Part I

Building CS Enterprise I

Chapter 2

Building process

In order to make CSE1 suitable for research and experiments, several upgrades and adjustments were needed. Creating for instance a DP systems for CSE1 calls for a way to precisely adjust the thruster set-points by a computer (DP controller). Therefore the original hobby remote setup needed to be removed as it can not be controlled by a computer. To replace the original hobby remote and transmitter, the Compact RIO 9024 from National Instruments (NI) was selected for this task. The Compact RIO 9024 is a high performance DAQ, with swappable C-series I/O modules. This allows for rapidly reconfiguration of the Compact RIO with C-series modules to have the proper interface for the designated sensor, actuator and so on.

When CSE1 was delivered to NTNU, it was taken for a test run by Torgeir Wahl. He discovered that the current bow thruster on CSE1 was not as powerful as anticipated. The original bow thruster was of the paddle blade type, a type with a reputation to be less effective than propeller types and very vulnerable to damages on the paddle blade. It was therefore recommended to replace the bow thruster by a more powerful propeller type bow thruster.

(a) The old bow thruster

(b) The old bow thruster removed.

(c) The new and improved bow thruster installed

Figure 2.1: Retrofit of bow thruster. The old bow thruster was cut out using a Dremel tool. Then the hole was furbished and cleaned before the new bow thruster was adjusted to fit the holes in the hull and glued on with epoxy.

After the new bow thruster was installed, the next step was to install the VSPs. Before that could be done, the old propellers, rudders, motors, and propeller shafts needed to be removed. The holes for the tail shaft tunnel was sealed up with epoxy glue, and reinforced with a small plastic plate to provide better structural integrity. The VSPs were delivered with round "base plates", and these were used as templates to aid the process of deciding where to place the VSPs. The ideal place to mount the VSPs would be on a completely flat surface (to gain greater connection area, and thereby increase the strength, and minimize the possibility of water leaks), but the stern of CSE1 has a rather curvy surface.

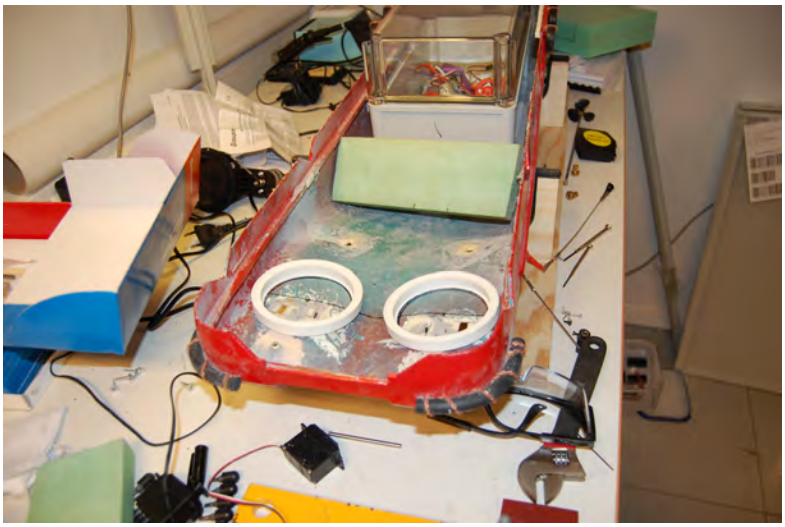

Figure 2.2: Selected placement of the VSPs. The white "base plates" indicates where the holes for the VSPs will be cut. Measure twice, cut once!

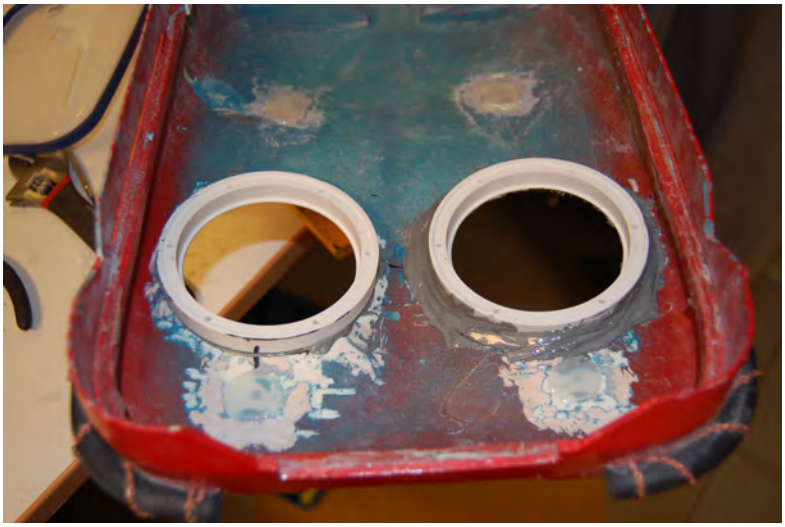

Figure 2.3: The holes cut, and the "base plates" for the VSP glued to the hull. More glue was added later to increase the structural integrity.

After the epoxy had harden, the actual VSPs were placed in the "base plates" and attached with screws. In between the "base plates" and the VSPs rubber sealing was placed in order to avoid water leaks.

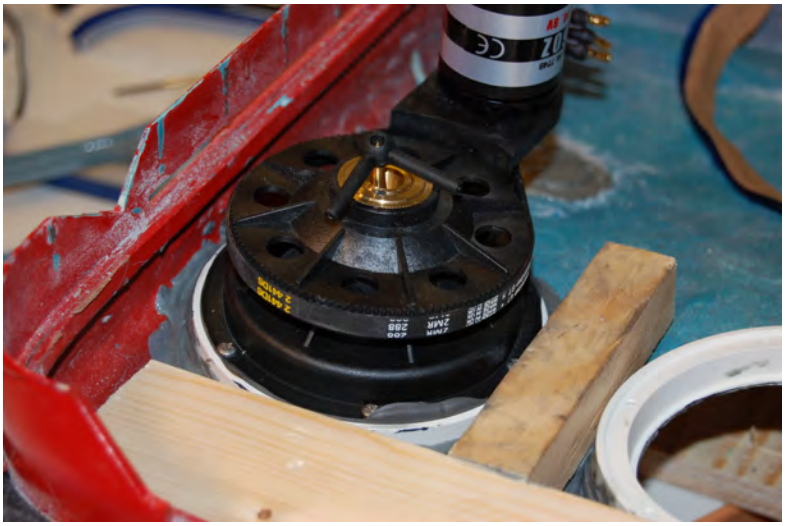

Figure 2.4: Port VSP attached to its "base plate". Notice the rubber seal being slightly squeezed out between the VSP and its "base plate".

After all these modifications to the hull, CSE1 was wet tested to check for leaks. CSE1 was put on the water, and two lead weights, each weighing $5kg$ were placed in the hull

for ballast. This ensured that the desired draft was reached, submerging all the newly created seals in the hull. CSE1 was left in the water for about 15 minutes under close supervision, and no leaks were detected.

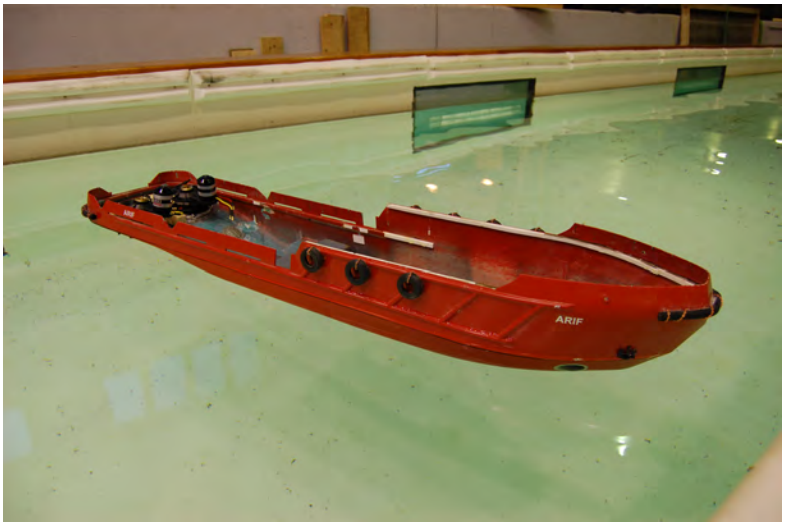

Figure 2.5: Wet testing to check for leaks on CSE1

The inner hull of CSE1 was painted with white spray paint. This was done purely for esthetic reasons.

(a) Masking up the VSPs before painting

(b) Masking up the bow thruster

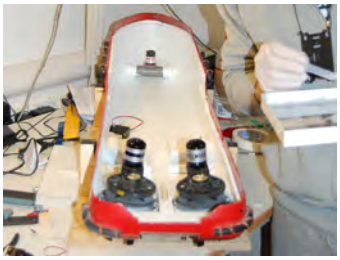

(c) The final result after the paint has dried, and maskings removed

Figure 2.6: Painting the inner hull of CSE1

The thrust direction of the VSPs is given by the position of the control rod on the VSPs. In order to control the position of the control rod, two hobby servos for each control rod were used. This allows for movement of the control rod in its entire "operating region", i.e. the mechanical space which the control rod can be located in. A condition for this to be true is that the servos that is connected to the control rod has an arm (between

the “swing wheel“ on the servo and the end of the “control rod“) , so that a rotating a servo gives a translation of the control rod. Also the servos needs to be mounted approximately normal to each other, and in approximately the same height as the top of the control rod. To achieve this, a mounting plate in wood was custom made to house the servos. The mounting plate was attached with screws to support plates glued to the hull. The ”arm“ between the servo ”swing wheel“ and the control rod, is screw threaded, and the connectors on the ”swing wheel“ and control rod is tapped. This makes the arm a simple turnbuckle that allows for adjustments of the arms length.

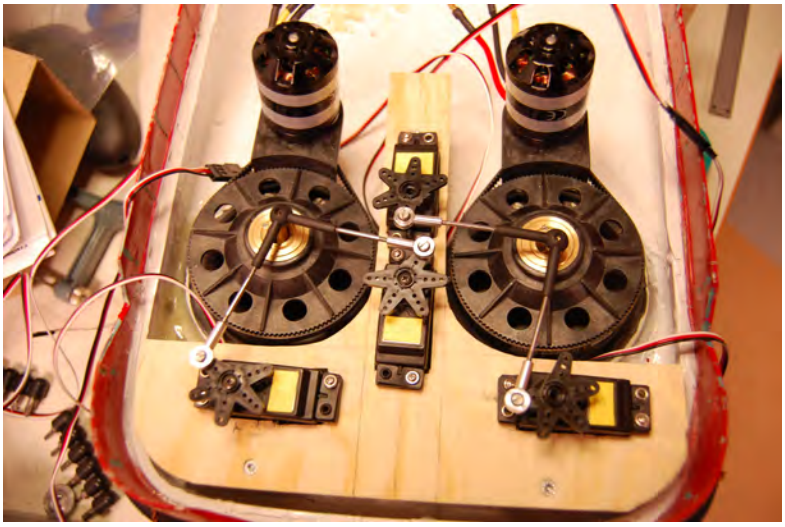

Figure 2.7: Servos mounted in their mounting plate, and mechanically connected to the control rod on the VSPs.

The servos were wired up for a small test to demonstrate that they could easily change the position of the control rod. The test was a success. Then the work of mounting the waterproof box to house the electronics started.

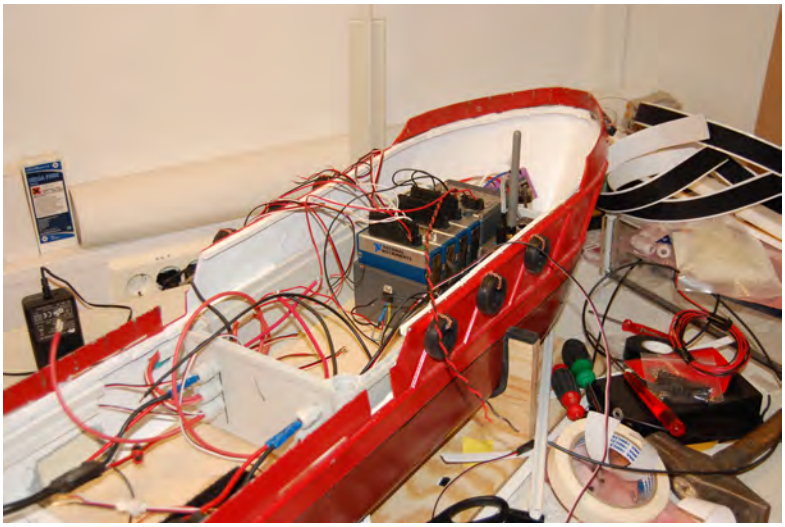

Figure 2.8: Mounting the Compact RIO in the waterproof box completed, and wiring in progress.

After the test where CSE1 was put in the water to check for leaks, it became clear that a larger freeboard was needed. The current freeboard was only $2cm$ at its lowest, and water could easily get into the ship at this point, especially in the presence of waves. Even though the Compact RIO is protected by the waterproof box, other parts such as the VSPs could still take damage by water. A solution to this problem was to glue on a plastic moulding to the sheer rail in the aft of the ship. This increased the freeboard to about $7cm$ around the entire ship. A deck was made out of high density plywood. The deck spans the way all around the ship, and its purpose is to increase the strength of the hull as well as serve as a base for a lid that could be put upon the entire ship.

The main battery and bow thruster battery is secured to the ship by Velcro tape. This makes it easy to take inn and out the battery for charging. Also the Compact RIO and the WiFi adapter located in the waterproof box is secured with Velcro tape. This way it is easy to change the position of the equipment to fine trim the ship. Cable ducts were fitted inside the hull between the servos and the waterproof box, and between the bow thruster and the waterproof box.

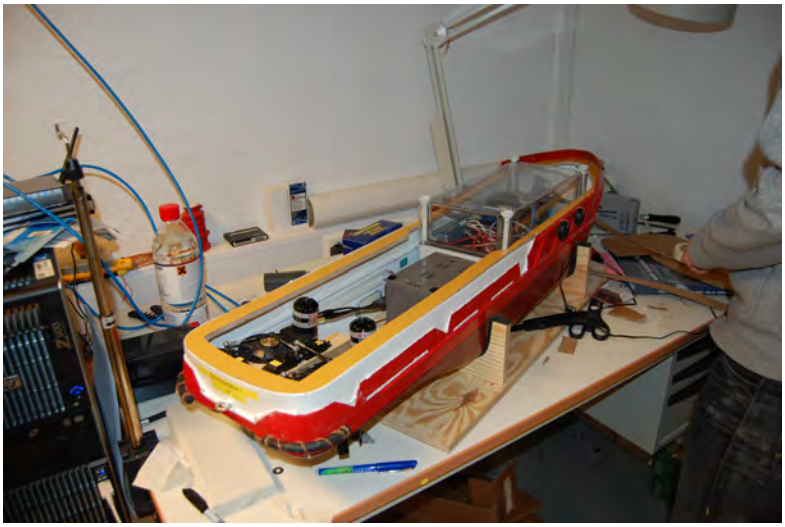

Figure 2.9: The improved freeboard and deck finished

After all the components were installed in CSE1, the cabling process commenced. The basic concept is that the Compact RIO and the Electronic Speed Controls (ESCs) for the VSPs are powered by the main 12V battery, and the WiFi adapter and bow thruster are powered by the auxiliary 6V battery. The reason why everything is not powered by the same battery is that the Compact RIO and the ESCs needs at least 9V to operate, and the ESC for the bow thruster and the WiFi adapter are rated for 5V. Further on the Compact RIO generates Pulse Width Modulation (PWM) control signals to all the servos and ESCs. See Figure 2.10 on the next page.

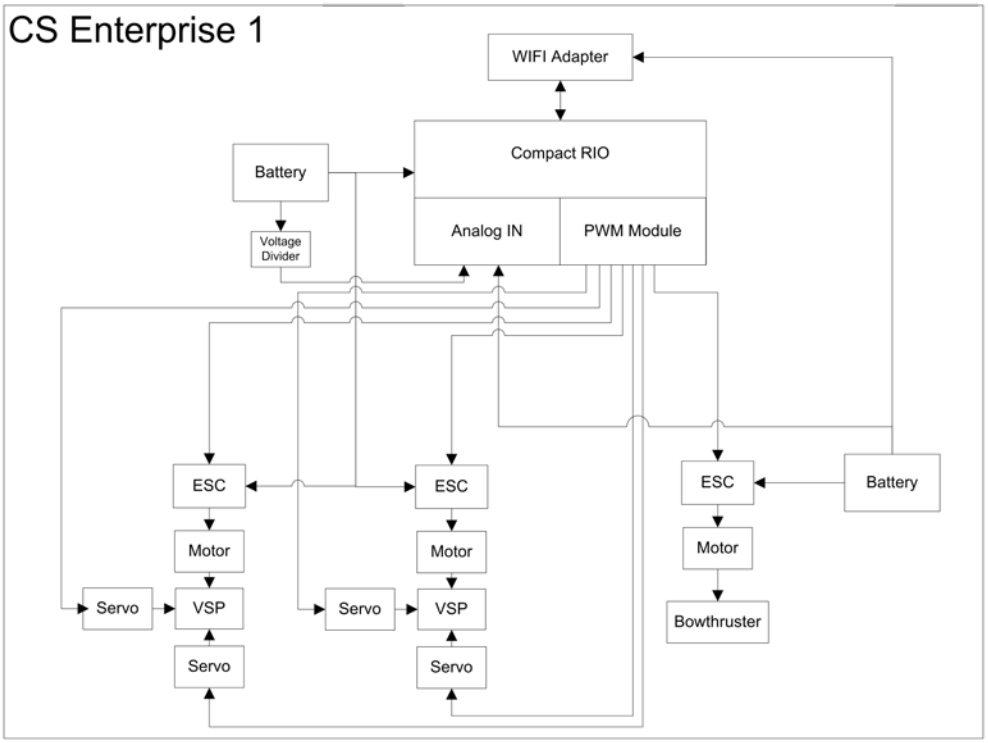

Figure 2.10: Topology of the wiering aboard CSE1.

Even for a rather simple setup, the amount of wiring was soon to become tremendous. To remedy on that a connection board was created, seen in Figure 2.11

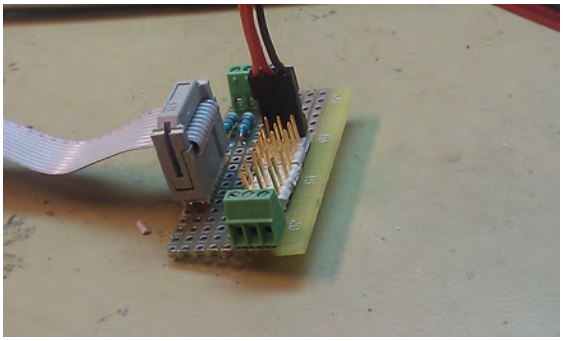

Figure 2.11: Custom connection board made to reduce the amount of wiring. The servo connectors goes on the brass pins, and the gray wire connects to the Compact RIO.

Chapter 3

Marin Cybernetics Laboratory

All the experiments carried out on CSE1 will be conducted in the MC Lab at NTNU. The peremises where the MC Lab is located today were originaly a storage tank for model ships from back in the days when the ship models were made out of parafin-wax and needed to stay wet. In 1990s this storage basin was transformed to a high tech test facility for the marine cybernetics branch of science. The founding of the MC Lab was done by NTNU, but with support from several industry partners such as *The Norwegian Shipowners Association*[1], *The Research Counsil of Norway*[2], *DNV*, *Statoil*, *MARINTEK* and *SINTEF*.

The MC Lab is an experimental facility for testing of ships, rigs and underwater vehicles. The basin has dimensions $LxBxD = 40m\ x\ 6.45m\ x\ 1.5m$ and is equipped with a towing carriage that can be towed at 2.0 m/s and move in 5 Degrees Of Freedom (DOF). A wave generator capable of generating waves with waveheights $H_s = 0.3m$ and periods $T = 0.6...1.5s$ (irregular waves) is located at the end of the basin, and plans for installing current and wind generators exists [Norwegian University of Science and Technology, 2010].

[1] In norwegian: Norges Rederiforbund
[2] In norwegian: Norges Forskningsråd

Figure 3.1: The basin and towing carriage in the MC Lab

To measure position and orientation of a vessel, the MC Lab is equipped with the *Qualisys Motion Capture System*. This is an optical system that uses special Infra Red (IR) cameras to track IR markers. The markers are spheres coated with an IR reflected material, and the IR cameras have an inbuilt IR flash. The setup in the MC Lab consists of three IR cameras placed on the towing carriage all faced towards the basin. CSE1 is equipped with a array of four IR markers, and at any given time at least two cameras need to be in clear line of sight to all four markers in order to compute the position and orientation of CSE1. The IR cameras are connected to a host computer inside the MC Lab that is running the Qualisys Track Manager (QTM) software. It is the software itself that calculates the position and orientation. The software can also control several different parameters for the cameras such as exposure length, flash intensity and frame-rate. The QTM software calculates position and orientation in real-time, and can pass on this real-time information over Ethernet(TCP/IP) to other computers and equipment.

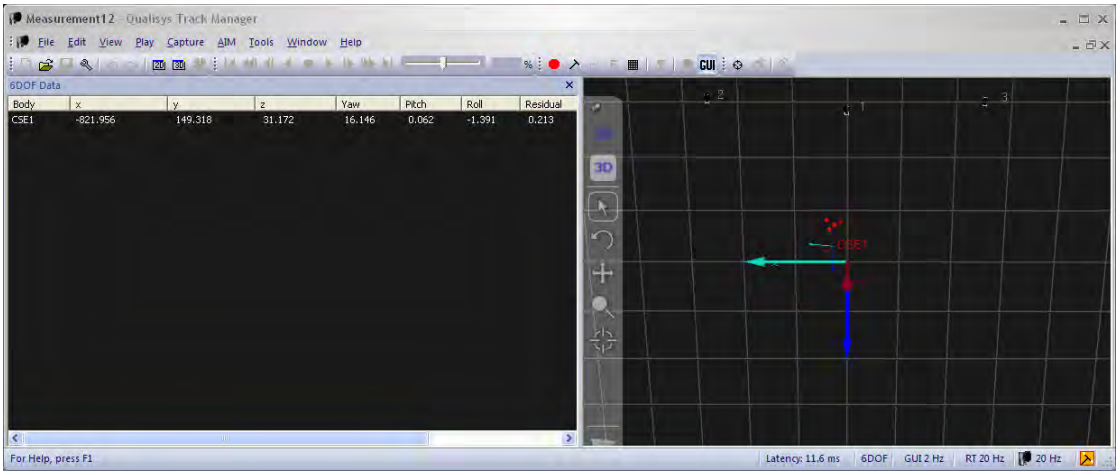

Figure 3.2: The QTM software. In the window to the left, the 6 DOF data for CSE1 is displayed. X,Y and Z are in millimeters relative to a coordinate system fixed in the basin. Roll, Pitch and Yaw are in degrees. The window to the right is the 3D window. The large arrows represent the fixed coordinate system, and the smaller arrows represent the position and orientation of CSE1. It is hard to see the notations on the arrows, but as for most 3D software, the notation were red,green, and blue represents x,y, and z respectively is also used here. The four red spheres in the 3D window indicates the position of the IR markers.

To control CSE1 the MC Lab has a dedicated computer running Windows XP SP3. This computer has the LabView software installed, and it will be used to create the Graphical User Interface (GUI) for CSE1. LabView is made by National Instruments (NI) and it is therefore well suited to use together with the Compact RIO aboard CSE1. LabView communicates with the Compact RIO over Ethernet. Having a cable attached to CSE1 in order to operate it would be impractical, and therefore CSE1 has a wireless Ethernet adapter aboard. The LabView computer is connected to a network with an access point, and can therefore communicate wireless with CSE1. The other computer running the QTM software is connected to the same network, and LabView can therefor obtain real-time position and orientation data from the Qualisys system.

LabView is a widely used software in the industry. LabView allows for rapid prototyping as well as creation of more permanent control systems. The major advantage of LabView is that it uses a graphical "drag and drop" interface to build applications. This way the user can easily create GUIs and powerful logics without having to know a low level programming language (such as C/C++)[3].

Even though LabView is considered very powerful and would in our case meet all our

[3]It can discussed whether C/C++ are low-level languages or not. In the classical sense, they are high-level, but relative to todays standards they can be classified as low-level languages

needs regarding functionality, a lot of users still swear to the Matlab/Simulink SW. Any discussion regarding which is better will be omitted here, but the fact is that marine cybernetics students at NTNU is a lot more familiar with Matlab/Simulink than LabView. Therefore, the LabView add-on named *Simulation Interface Toolkit (SIT)* is available at the MC Lab. This add-on allows the user to create Simulink models that can be interfaced with LabView. If real-time workshop is available in addition, then SIT can use the code generated by real-time workshop to compile code into binaries that can run directly on the Compact RIO and its Field-programmable gate array (FPGA) module. Simulink models running as binaries directly on the Compact RIO / FPGA runs a lot faster than native Simulink models (on for example Windows/Linux). This boost in execution speed is an important aspect of preserving the real-time capabilities of the system. If the deadlines in the code are not met due to high execution time, then the system will loose its real-time capabilities.

To do manual control of CSE1 a PlayStation 3 (PS3) hand controller is used for user input. The PS3 controller communicates with the computer wireless over bluetooth. Chapter 5 will reveal more details about this controller. It is only presented here as it is consider a part of the MC Lab.

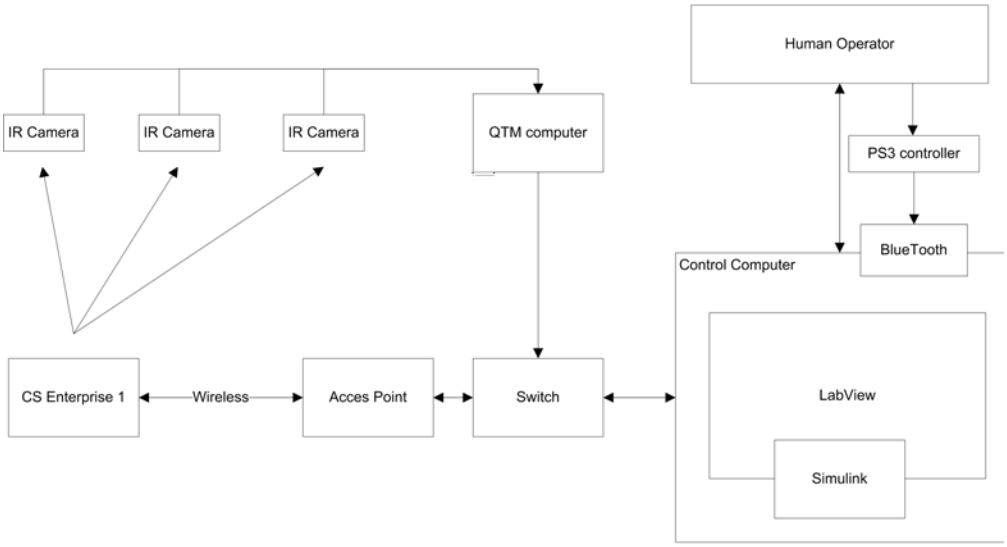

Figure 3.3: Topology of the HW and SW in the MC Lab releated to CSE1.

Chapter 4

Voith Schneider Propeller

Figure 4.1: A real world VSP [Courtesy: Voith Turbo, 2010]

4.1 History and background

The VSP was invented by the Austrian inventor Ernst Schneider, and developed by the Voith company. The invention dates back to the late 1920s. In 1928, the first prototype VSP was installed in the experimental vessel *Torqueo*. The VSP aboard the ship was powered by a 60 horsepower engine [Jürgens and Fork, 2002]. The *Torqueo* demonstrated great maneuvering capabilities, as it could change the thrust direction from the VSP almost instantaneously, and the invention was considered a technical triumph.

Due to the great maneuvering properties of a ship equipped with VSPs, the VSP became a popular propulsor on ferries and tugs. Ferries and tugs often operate in confined waters, and therefore the ability to maneuver swift and safely is highly appreciated. Already by 1933, Voith had produced 80 VSPs, primarily for ferries and tugs. During the Second World War, the VSP was produced in a great number, and the majority of the produced propellers were installed in German minesweepers. Today, the majority of the produced VSPs are still installed on ferries and tugs. The rest of the ships equipped with VSPs are typically "special ships".

The VSP has not been extensively used for DP vessels [Bray, 2003]. The ability of changing the thrust direction almost instantaneously should be a desirable feature for all DP vessels. A much more common propulsor for DP vessels today are azimuths. Doing a full crossover in thrust direction for such a propeller might take up to 30-60 seconds for a large ship. The VSP's ability to change thrust direction almost instantaneously makes it possible to use the VSP for active roll damping. [Jürgens and Palm] has also found that the slamming pressure on hulls with VSPs is reduced compared to hulls with azimuths, and that the VSP is much less subjected to cavitation than azimuths.

On the other hand, one of the disadvantages of the VSP is that its efficiency can not match up with conventional propellers at high speeds. But it has been demonstrated that the VSP had higher efficiency than Contra-Rotating Propellerss (CRPs) in some cases [Marine, 2005]. Another drawback for the VSP is that the total capital expenditure of equipping a ship with VSPs are significantly higher than other propulsors such as azimuths. This is related both to the procurement itself, and other expenses that follows such as additional required steel work on the ships hull. Despite the higher expenses associated with the VSP one might ask oneself why the VSP have not gained more popularity on DP vessels. In 2003 the shipping company *Østensjø Rederi* launched "Edda Fram", the first Platform Supply Vessel (PSV) operating in the North-Sea to have VSPs. "Edda Fram" is a DP class 2 vessel (DYNPOS- AUTR), and the DP system also incorporates an active roll damping system by using its VSP. Tests performed on "Edda Fram" show that the significant roll angle can be reduced from 8 degrees to 2 degrees in irregular waves with zero mean crossing frequency of 15 seconds, wave height of 3 meters, and metacentric height of the vessel of 1.3m [Marine, 2005].

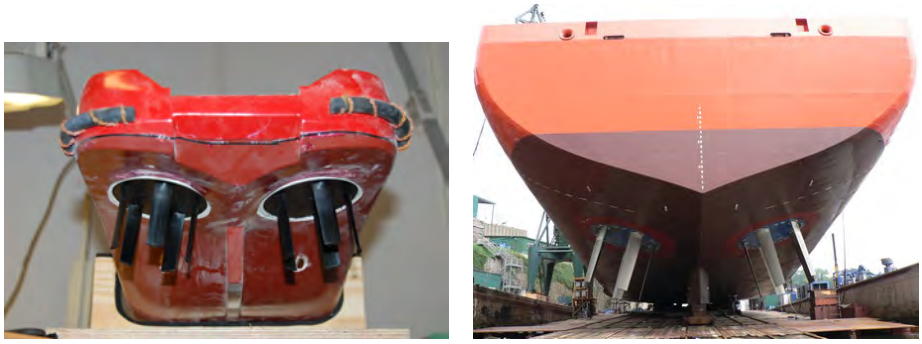

(a) CSE1 (b) Edda Fram

Figure 4.2: The VSPs on CSE1 and Edda Fram compared. By studying these photographs, it becomes clear that the relative size of the VSPs on CSE1 is significantly greater than the VSPs found on Edda Fram. [Picture (b) Courtesy: Østensjø Rederi, 2010a].

"Edda Fram" paved the road for "Østensjø Rederis" next vessel to be equipped with VSPs, the "Edda Accommodation". "Edda Accommodation" is a multipurpose service and accommodation vessel, and it is currently being built in Spain. The ship will have five VSPs, three in the stern region and two in the bow region.

Figure 4.3: Render of Edda Accommodation. Note the three VSPs in the stern, and the two in the bow.[Courtesy: Østensjø Rederi, 2010b]

4.2 How it works

The VSP consists of a rotating blade wheel with a vertical axis of rotation, and a number of blades mounted in a circle parallel to the axis of rotation. The blades are projected downwards into the water and are mounted on a rotor casing that ends flush with the ships bottom. To generate thrust, the blades must be pitched outwards in the first half of their rotation and inwards in the second half. They must therefore perform an oscillating motion while they rotate in a circle. The pitch of the blades are constantly adjusted along one rotation to obtain optimum effect from the blades [Jürgens and Fork, 2002]. The pitching mechanism is designed such that the normals of all the blades intercept each other at the same point at any given time. Hence the resulting thrust direction of the VSP is given by the intersection point of the normals. To adjust the intersection point of the blade normals, and hence the thrust direction and magnitude, the VSP has a control rod that is connected to the blades through a mechanical linkage system. Adjusting the position of the control rod changes the pitch of the blades, and hence the thrust direction. The control rods position is normally controlled by hydraulic actuators. Observe that if one demands thrust in a given direction, then the control rod must be placed ± 90 degrees relative to that direction depending on which way the VSP is rotating. See figure 4.6 on page 24.

The design of the VSP allows for no thrust generation even at full blade wheel speed. This is done by setting no pitch on the blades, i.e. the angle of attack for all the blades is zero during their entire rotation. In this case the intersection point of the blade normals will be in the center of the blade circle. To clarify the principles of the VSP further the following pictures will be used to demonstrate.

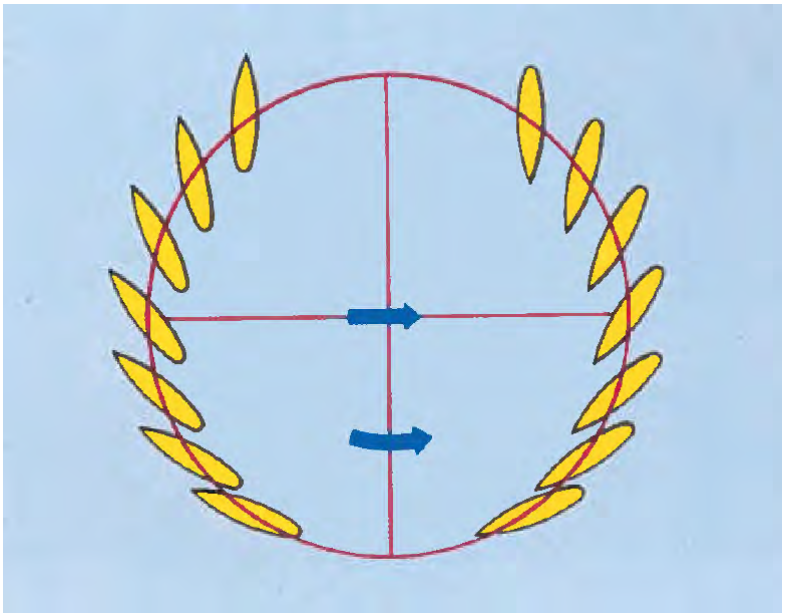

Figure 4.4: Forward thrust from the VSP as it rotates. Note that the blades are turned inwards in the first half of their rotation, and outwards on the second half. [Courtesy: Jürgens and Fork, 2002]

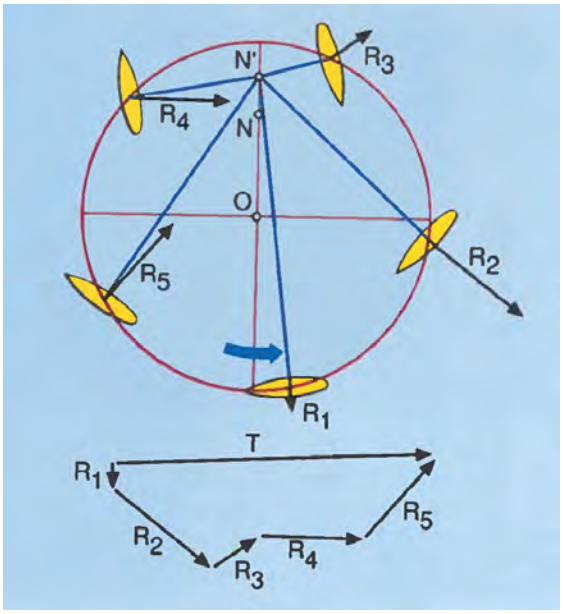

Figure 4.5: Hydrodynamical forces. R_1 to R_5 are the hydrodynamical forces generated at each blade when the insercion point of normals is at the point N' and the blades are rotating in the direction of the blue arrow. Summing up these hydrodynamical forces gives the resulting thrust vector $\boldsymbol{T}$. [Courtesy: Jürgens and Fork, 2002]

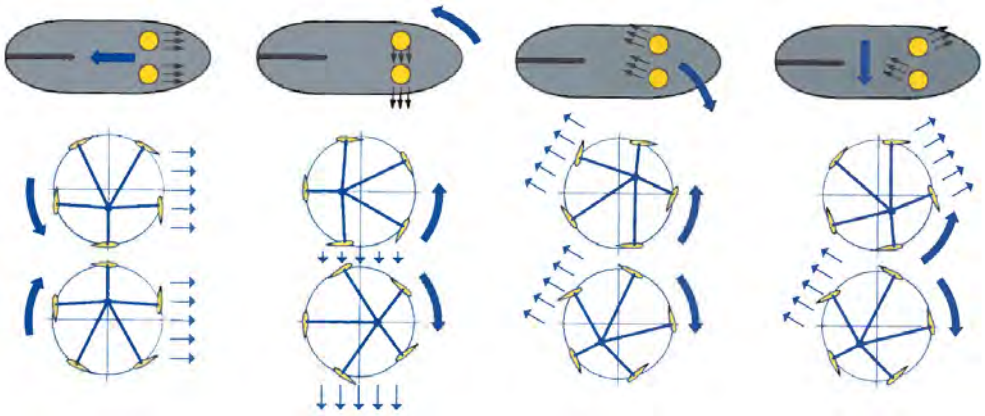

Figure 4.6: Typical setup and operation for a tug boat with two VSPs. The thrust direction is given by the position of the control rod, that controls the interception of normal point. [Courtesy: Jürgens and Fork, 2002]

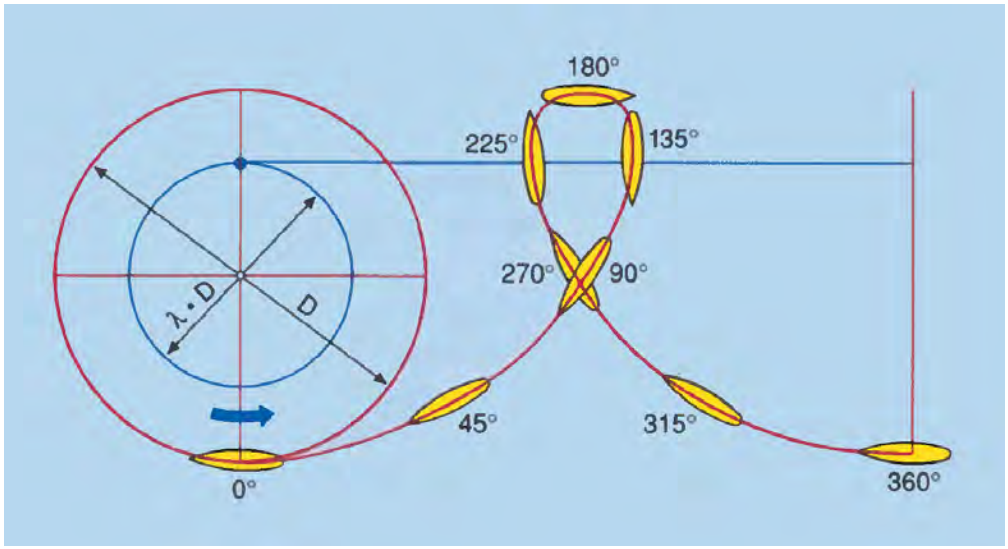

Figure 4.7: The VSP blades describes a cycloidal path through the water. In this figure it is shown for zero thrust operation. [Courtesy: Jürgens and Fork, 2002]

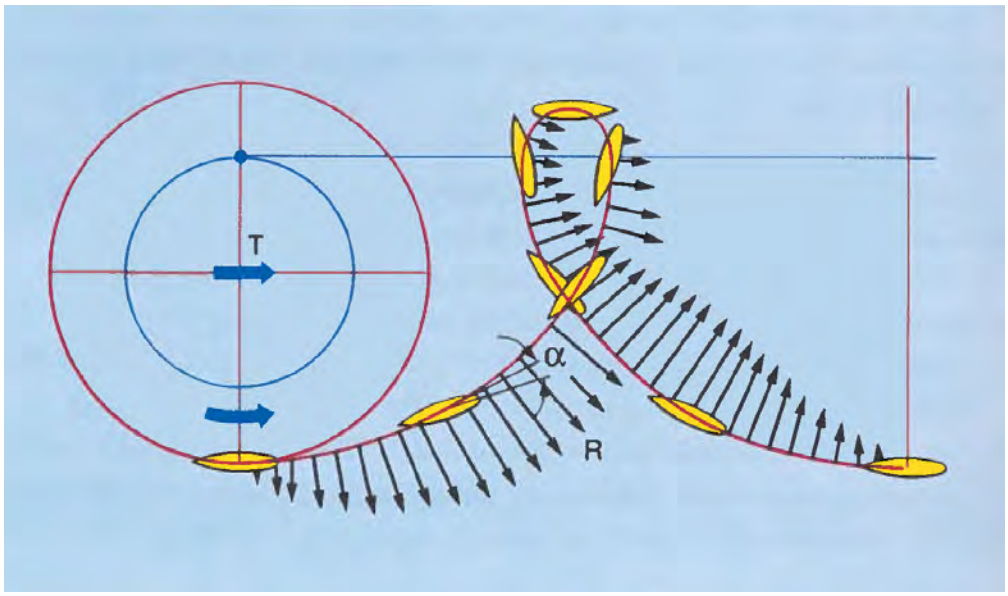

Figure 4.8: Path of the VSPs blades through water when generating thrust. The blades are turned through the angle α on their paths. R denotes the hydrodynamical force at the blade, and $\boldsymbol{T}$ is the resulting thrust. [Courtesy: Jürgens and Fork, 2002]

The VSPs installed in CSE1 works the same way as for a real ship, and utilizes the same basic principles. The VSPs for CSE1 are manufactured by the Graupner company, and

according to Graupner the model VSP is developed with the help of original factory drawings. Their marketing wording sounds:

> True-scale propeller drive unit for powering and controlling model boats. The new Voith-Schneider propeller unit (usual abbreviation VSP) for model boats was developed with the help of original factory drawings. At the design stage we insisted that all the basic functions should emulate those of the original. In the Voith-Schneider system the propeller generates both thrust and steering forces by altering the angle of the propeller blades [Cornwall Model Boats, 2010].

Figure 4.9: Model scale VSP that is installed in CSE1.[Courtesy: Cornwall Model Boats, 2010]

The major difference between the model scale VSP and the real world VSP is that the blades on the model VSP has a symmetrical profile so that it can be configured to rotate both clockwise and counterclockwise. Real world VSPs, however, have blades that are optimized for one rotational direction only. VSPs are often installed in pairs, and configured to rotate in the opposite direction to each other. Another difference is that the control rod on the model VSP is controlled by hobby servos, where the real world VSP uses powerful hydraulics actuators. This is due to size and practical aspects, and the different ways to position the control rod is non-essential in this context.

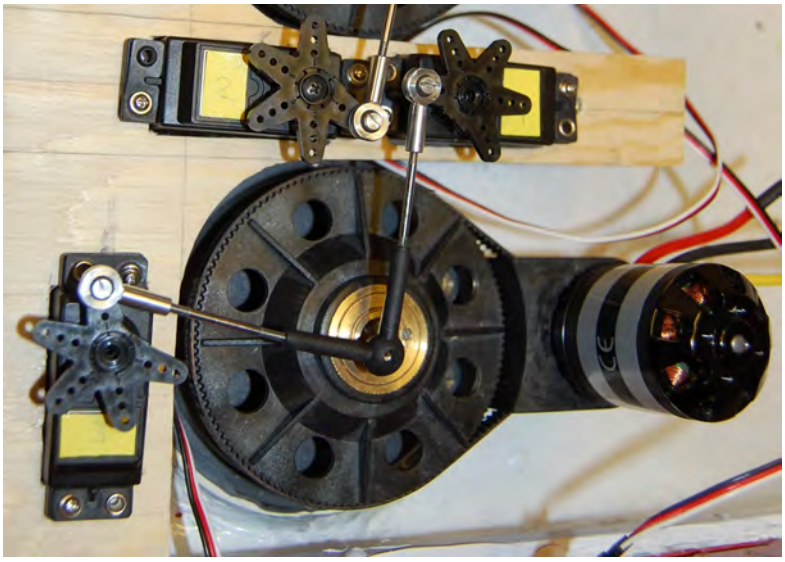

Figure 4.10: Close up photo of the port VSP and its servos controlling the control rod's position.

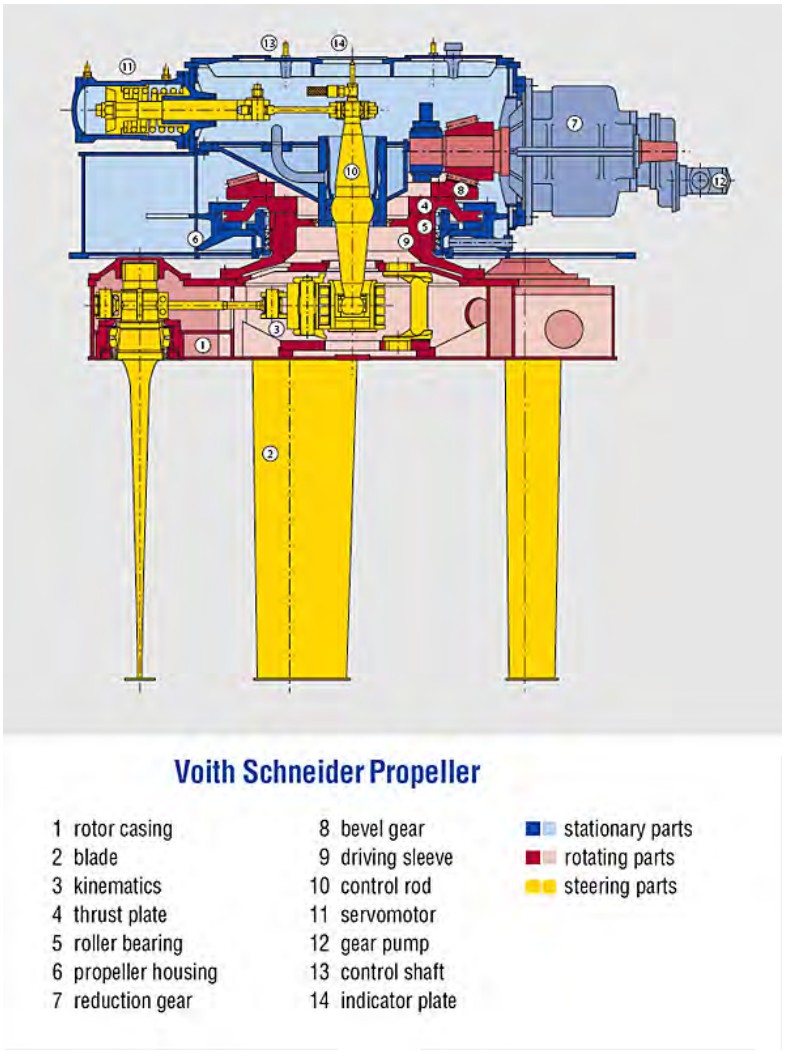

Figure 4.11: Longitudinal section through a VSP. [Courtesy: Voith Turbo, 2010]

Each VSP on CSE1 is powered by a *Graupner Compact 460Z* electric motor. Unfortunately there is no available datasheet for these motors specifying power and other parameters. Only a short specification found on Graupner [2011] that is listed in table 4.1 on the facing page. If one tries to calculate the power based on the specifications given in the table, assuming zero losses gives $Power = Voltage \cdot Current \rightarrow 14.8V \cdot 26A = 384.8W$. But it is hard to believe that this small motor can have such high power.

Table 4.1: Graupner Compact 460Z specifications

Specification
Nominal voltage: 14.8 V
Operating voltage range: 7.4 ... 18.5 V
No-load speed: 13,320
Revs. / Volt (kV): 900
Permissible motor direction: R and L
Case length excl. shaft approx. 46 mm
Diameter approx. 35.2 mm
Free shaft length approx. 18 mm
Shaft diameter approx. 4 mm
Weight approx. 164 g
Thrust in N (1 N = 100 g): 14
Current drain: 26 A
Connector type: G3.5

Each electric motor is controlled by a ESC. The ESC is powered by the main battery (12V Direct Current (DC)), and outputs a 3-phase Alternating Current (AC) voltage to the motors. A PWM signal is sent to the ESC to control the amount of power delivered to the motors. The PWM signal is obtained from the Compact RIO aboard CSE1.

Chapter 5

Manual thruster control

In the previous chapters CSE1 and the MC Lab have been presented. This chapter will describe how everything is put together to make a manual thruster control for CSE1, and hopefully put the previous chapters in a better context.

Before one starts to design for instance a DP system, it is important to verify that all the thrusters, communications and so on work properly. Especially in this case where CSE1 is a brand new model ship, and no one has any previous experience with the setup.

One of the first tasks that was done was to figure out how to control the VSPs. One already know that this is done by adjusting the position of the control rod, and that this is done by the two servos. But what still remains unknown is what kind of PWM signals that need to be sent to the servos to obtain a desired position for the control rod.

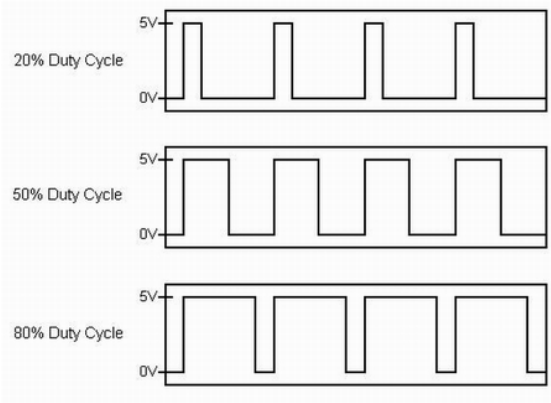

Figure 5.1: Pulse Width Modulation (PWM) signals with different duty cycles. [Courtesy: National Instruments, 2011]

The first part of this challenge was to figure out how the servos behaved, and what duty cycle in the PWM signals that corresponds to which servo position. For hobby servos the PWM signal frequency is $50Hz$. Each pulse is therefore 20 milliseconds, and the amount of time that the control signal is high within each 20 millisecond frame controls the servo position. Unfortunately there was no data-sheet shipped with the servos indicating what pulse widths that corresponds to the servos positions. Therefore this would be an exercise in "reverse engineering".

The PWM signals will be generated from the Compact RIO. The Compact RIO was configured to output a PWM signal at $50Hz$, controlled by a virtual control in LabView. Also for this part had no documentation was provided about the generated PWM signal. It was only possible in LabView to set a double numerics as set-point for the PWM signal. If this numeric was the pulse width in absolute time, percentage of "time high" or a scaled output (ranging from 0-1 for instance) was not known.

With no documentation about the servos and the properties of the generated PWM signal, it was therefore hard to design a control signal based on "first principles". A trail and error approach was started. A spare servo of the same type as the ones found in CSE1 was wired up to the Compact RIO. A spare servo was used such that the servo could have unrestricted movement over its entire operating range. The servos connected to the control rod of the VSP is restricted in movement due to the mechanical saturation limits of the control rod. Then the control signal in LabView was adjusted to see what signal ranges that gave movement on the servo. It was found out that the servo responded to control signals in the approximately range 0.01 to 0.09, where 0.01 corresponded to -90 degrees and 0.09 corresponded to $+90$ degrees.

With this as a starting point, a mapping for the control signals to the servos could be designed. To make it easier to design this a coordinate system for the position of the control rod was chosen. The idea is to have a function where the input is the desired control rod position, and the output is the numerical value of the PWM signals sent to the servos.

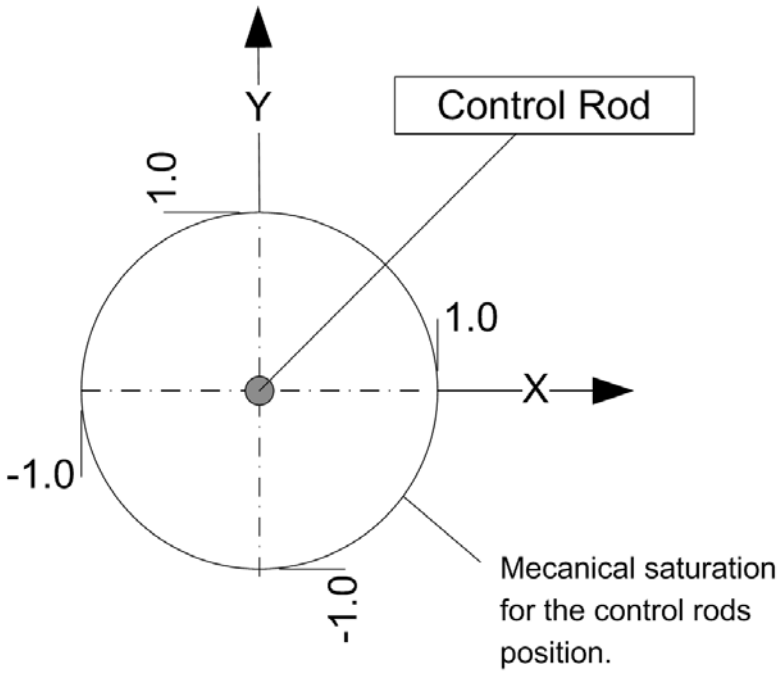

Figure 5.2: The chosen coordinate system for the control rod. In this coordinate system, the X axis is in the ship's longitudinal direction, from aft to fore, and the Y axis points to port on the ship. The reason for this choice was because only 2D was considered, and because it was logical when working on CSE1. In hindsight the coordinate system should have been chosen according to the SNAME notation in order to avoid confusion.

Because the servos are not aligned up such that a servo movement gives a straight line movement of the control rod parallel with the ships axis, some sort of mapping function is needed. In addition, turning only one servo will give a slightly curved movement of the control rod position, because the control rod will rotate about the other servo.

Several different approaches for creating the mapping function for the VSPs were considered. The first attempt was to consider the entire mechanical system of the servos, rods from servos to the control rod and the control rod as a mechanical linkage system. In figure 5.3 on the next page the approach is presented on a four bar linkage. In the figure, point O and point C will correspond to the centers of the swing wheel on the servos, i.e. the points the servos rotates about. The lines OA and CB corresponds to the swing wheel itself. The lines AX and BX are the arms connected to the control rod, which in this case corresponds to X. Note that the line AB is no physical mechanism on the actual servo setup, but for the linkage theory this bar constrains the angle AXB. The reason for modeling the servo system as a mechanical linkage is that the mechanisms are

quite similar, and a lot of theory already exists on the topic. However, this approach was rejected for several reasons. First of all, the gripping that connects the arms from the servos to the control rod is flexible. This means that the angle AXB will not be fixed in the mechanical linkage analogy. The basic theory for mechanical linkages assumes that all the bars have infinite stiffness, and hence the theory will not be applicable. However, theory for flexible bars exists, but then the computations would be much more complex, and the advantage of models this problem as mechanical linkages would be lost. Another drawback that was first discovered after trying to set up a model using mechanical linkage theory is that the point X in this case will not be free to move in the entire operating range of the control rod. Again, due to the assumption of infinite stiff bars, the point X is restrained to only move in a path given by the geometry of the bars.

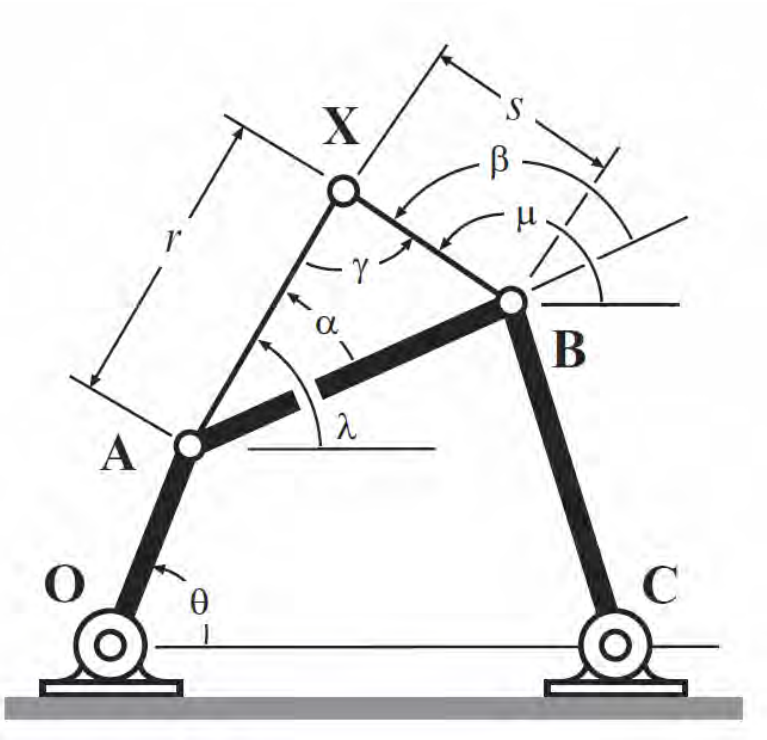

Figure 5.3: A four bar mechanical linkage [Courtesy: McCarthy and Soh, 2010]

When the approach of using mechanical linkage theory was finally rejected, another approach was tried. This time it was assumed that the gripping between the servo arms and the control rod was free to rotate, and based on that assumption a mathematical model based purely on the geometry was created. When the geometry (position of the servos, length of the servo arms and so on) are known, and the servo angles are known, then one should be able to compute the position of the control rod. The result was that one ended up with a large equation where position was a function of the angle. In order to use this the equations needed to be rewritten such that the angle was a function of the

position. Due to the extend of the equations, this was found nearly impossible. Another drawback with this approach is that the geometry would have needed to be known high precision. Any deviations in measured geometry could lead to a wrong placement of the control rod.

With two approaches to create a mapping function that had failed, it was time to rethink the strategy. After two failed attempts, a better understanding of the mechanisms were obtained. For the third attempt the KISS principle[1] was used for inspiration.

The idea was to create the mapping function with the use of lookup tables. The servo wheels were detached from the servos, and an approximately center position for the servo rotations were found. Then the servo wheels were attached to the servos again so that the control rod was as close as possible to its center position. Then the control signals to the servos where fine tuned from LabView such that the control rod reached zero. The control signals sent to the servos when the control rod was in its center position were then noted. Then the control signals were carefully adjusted such that the control rod was placed "full pointing forwards" measured by eye, and again the control signals to the servos were noted. This procedure was repeated for the coordinates showed in Table 5.1 and Table 5.2

Table 5.1: Control rod positions and corresponding control signals for the servos for port VSP.

Control rod position		Servo control signal	
X	Y	Servo1	Servo2
0	0	0.052446	0.047724
0	1	0.054152	0.057000
0	-1	0.049536	0.038609
1	0	0.043301	0.050095
-1	0	0.060000	0.045994

Table 5.2: Control rod positions and corresponding control signals for the servos for starboard VSP.

Control rod position		Servo control signal	
X	Y	Servo1	Servo2
0	0	0.054131	0.049747
1	0	0.055649	0.040388
-1	0	0.005396	0.060287
0	1	0.044266	0.052613
-1	0	0.0640809	0.047048

[1]KISS is an acronym for "Keep it simple stupid". The acronym was first coined by Kelly Johnson, lead engineer at the Lockheed Skunk Works (creators of the Lockheed U-2 and SR-71 Blackbird spy planes, among many others) [Rich, 2011].

The data in Table 5.1 on the facing page and Table 5.2 on the preceding page where then used to create a lookup table in Simulink. The lookup table was set to use linear interpolation, such that control signals for the servos could be calculated for all possible desired control rod positions. A small test where the lookup-tables were used to compute the control signals for the servos were conducted. The test revealed that with this implemented it was easy to obtain the desired position for the control rod on the VSP.

After the the control of the control rod position had been figured out, the ESCs were programmed. The ESCs is controlled by a PWM signal from the Compact RIO. To program the ESC it must be in programming mode. This is done by holding its push button for four seconds. Then a procedure, where the PWM signal is in sequence set to *neural-full ahead-neural-full astern*, and each set-point is confirmed by a button press on the ESC.

For the manual control, the user needs to be able to adjust the thruster set-points in an easy and swift manner. The easiest way to make such a Human Machine Interface (HMI) would be to make sliding bars or other forms of virtual controls in LabView. But this would be extremely hard to control, and require a skilled user. A *Logitech* PC joystick was available at the MC Lab, and had been used to control other model ships earlier. This joystick could of course be used, but it would lack the ability to control both VSPs and the bow thruster simultaneously. The perfect controller would be a controller where the user could operate all the actuators simultaneously. An option was to design a custom controller with several joysticks and sliders for instance, but such a solution would typically involve a lot of money and construction time. Then the idea of using a PS3 controller for input came up.

The PS3 controller has two thumb joysticks, each with a resolution of 16 bits, and several buttons where even some of them are steepless. By using the PS3 controller as input, the two joysticks could be mapped to the two VSPs, and the buttons for the index fingers could be set to control the bow thruster. As CSE1 is planned to be used for demonstrations and recruitment, the choice of the PS3 controller would be well suited as many young people are already familiar with this controller. Another positive aspect with the PS3 controller is that it is cheap, compared to other solutions. Today the PS3 controller has a retail price of around $400NOK$. The PS3 controller uses the bluetooth wireless protocol, and has a standard Universal Serial Bus (USB) plug for charging. The only problem with the PS3 controller is that it is designed only to work with the PS3 console. However, after some research it was found out that several people had posted software and tutorials on the internet on how to get the PS3 controller working with a Windows computer. The procedure described by [Lim, 2011] was used. This involved installing several drivers, and SW, and after a while Windows recognized the PS3 controller as a device. The main program that handles the connection of the PS3 controller is the BtSix, seen in Figure 5.5 on the following page. During the time spent in the MC Lab, the PS3 controller has already drawn a lot of attention, especially from the ”PlayStation generation“.

Figure 5.4: The DUALSHOCK 3 PS3 controller [Courtesy: komplett.no]

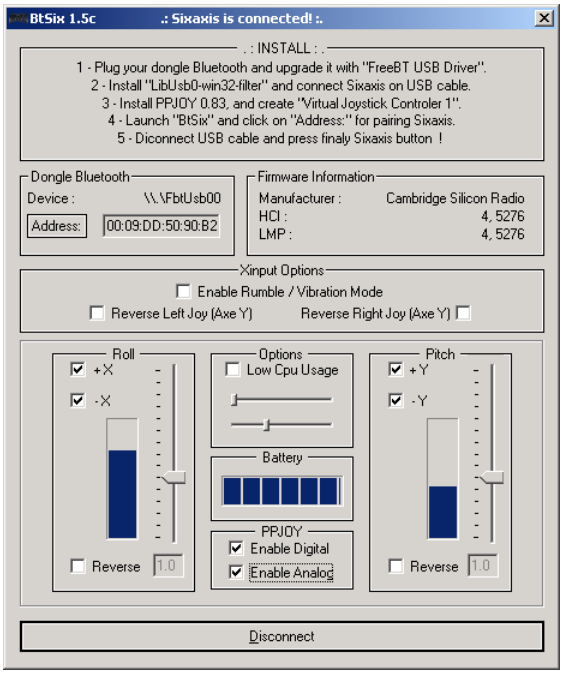

Figure 5.5: BtSix 1.5c screen dump

After the PS3 controller was recognized in Windows, it needed to be interfaced with LabView. LabView has inbuilt routines to interact with mouse/keyboard and joysticks, and these were used. On top of that, a GUI was created in LabView, to present various information to the operator. The GUI can be seen in Figure 5.6 on the next page, and the functionality is described below.

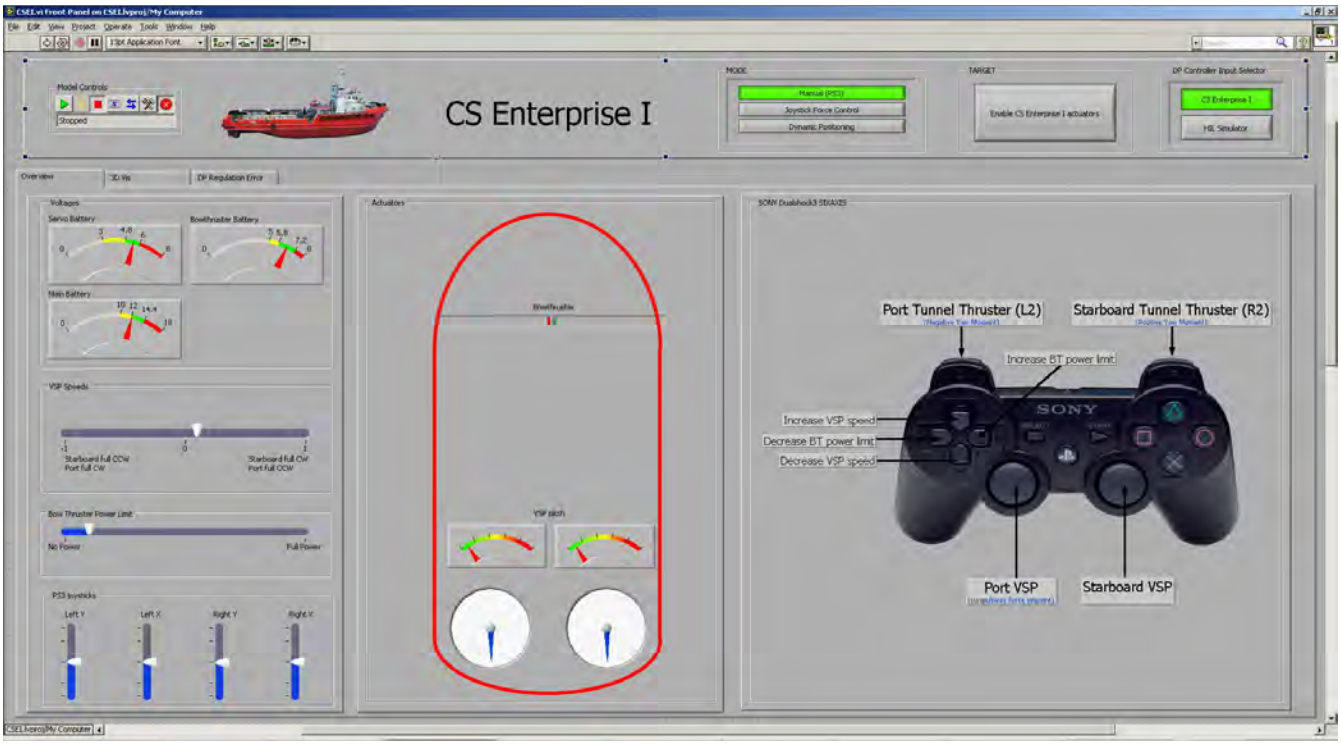

Figure 5.6: The main screen of the GUI

Model Controls After the LabView program has been started, these controls controls the Compact RIO and its state. To start execution of the code loaded on the Compact RIO, press play. To stop the Compact RIO from running, press the square stop icon. To only stop the GUI from running, the round "X" button can be pressed. This action does not affect the Compact RIO state. The "Model Controls" buttons are auto generated by LabView.

Voltage simply shows the voltage of the three on board batteries.

VSP speeds is an indicator for the speeds of the VSPs. To set the VSPs speeds, the right and left D-pad buttons on the PS3 controller must be used.

PS3 joysticks indicate the positions of the two joysticks on the PS3 controller.

Actuators show the state of the actuators in any operational mode for CSE1. The bow thruster set-point is indicated by a green bar proportional to the thrust set-point towards starboard, and similarity a red bar for port. The blue arrows indicates the thrust direction of the VSPs. The arrows are pointing in the wake direction. The gauges above indicates the relative pitch of the VSPs.

Sony Dualshock3 SIXAXIS describes the functions of the PS3 controller to the user, as well as indicating user actions on the PS3 controller. If a button is pressed, this is indicated by a green outline of the button. This functionality is neat to have to verify that the PS3 controller is connected properly.

Some of the buttons are not explained here, and these buttons have functionality related to the DP system, and will therefore be presented in Part II.

Sea Trials

When the building and SW were ready, it was time to take CSE1 out for "sea trials". All the systems had been thoroughly tested on land. The rotation speed could be adjusted, the pitch of the VSPs could be changed, the bow thruster was working and so on. However, one knew little or nothing about how the model boat would behave in the water, or if it was seaworthy at all. It was a great excitement related to the actuation properties of the VSPs. How much thrust would they generate, and will it be adequate for the vessel, or will the model VSPs even function at all?

It soon proved that the VSPs were able to produce a great amount of thrust. Running the VSPs at full rotational speed the thrust generated seemed way out of proportion compared to the size of the ship. At 40% of full power, the thrust generated from the VSPs seemed a bit more reasonable. The vessel was easy to maneuver, and after some short time of getting used to the controls, one could easily do advanced maneuvers such as driving sideways (pure sway motion), and rotate the ship around its own axis (yaw rotation). The easy operating of the ship was possible thanks to the PS3 controller. With this controller it proved possible to easily and precise adjust the thrust set-points, and also be able to control all the actuators simultaneously without having the needs to shift grip on the controller. The building of CSE1 and the manual thruster control was considered a great success. Other people not familiar with the vessel or the setup were allowed to try the manual control, and they all got a hold of it pretty fast.

Part II

Dynamic Positioning of CS Enterprise I

Chapter 6

DP model

Ships and vessels can be operated in many different ways, for example stationkeeping in offshore operations, seakeeping or transport of cargo and passenbers, rendezvous for replenishment at sea operations and so on. These different operational modes call for different mathematical models and parameters as the main physical properties will depend on how the ship or vessel is operated. This is also reflected in the controller design for these operational modes, as the controller design has to take the physical properties into account. On a top level, a vessel can be modeled as a 6DOF system, regardless of its operational mode. But such models can be too complicated to be used for controller design, or the parameters in the 6DOF model can be hard to obtain. Therefore, a mathematical model based on the operational mode is preferred. To further illustrate the different operational modes, and hence preferred types of models see Figure 6.1 on the following page. Unified models that are applicable to several operational modes do exists [Fossen, 2010], but such models are not in the scope of this report.

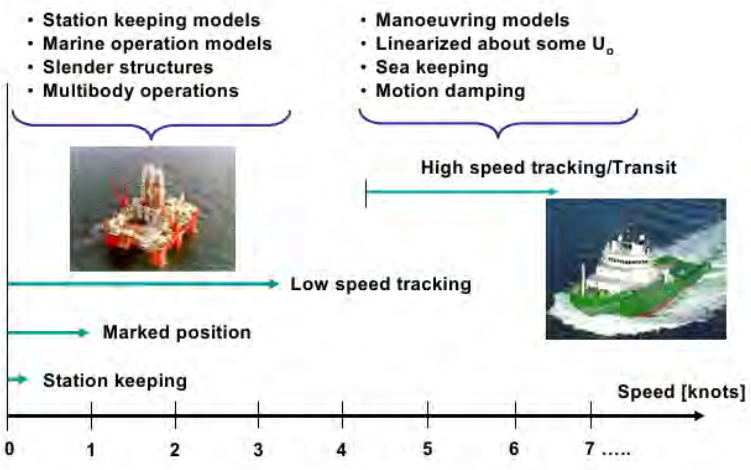

Figure 6.1: Modeling properties [Courtesy: Sørensen, 2005]

Modeling can be divided into control models, which are simplified models of the real world used for controller and observer design, and process models which are detailed models of the real world. Sørensen [2005] describes these models the following way:

Control model is a simplified mathematical description containing only the main physical properties of the process or plant. This model may constitute a part of the controller. The control model is also used in analytical stability analysis based on e.g. Lyapunov stability and passivity.

Process model is a comprehensive description of the actual process and should be as detailed as needed. The main purpose of this model is to simulate the real plant dynamics. The process model is used in numerical performance and robustness analysis and testing of the control systems.

6.1 Reference frames

In order to establish different mathematical models, different reference frames are needed. Several different reference frames exists, but only the two reference frames applied in this thesis will be presented.

NED: The North-East-Down reference frame. The origin of this frame is located at the surface of the Earth with coordinates determined by two angles (l and μ) denoting the longitude and latitude. Its x-axis is pointing towards true North, y-axis towards East, and z-axis pointing downwards and normal to the Earth's surface. For local

navigation of vehicles, close to the surface, it is common to assume that this frame is inertial, and that the coordinates of the vehicle is given in the xy- plane (tangential plane) of the NED frame (flat Earth navigation) [Skjetne, 2005]. The NED frame in this context will have its center in the centre of the basin at the MC Lab, and North pointing in the longitudinal direction of the basin.

Body: A reference frame fixed to the body of the vehicle. For a marine vessel the origin of this frame is usually chosen in the principal plane of symmetry with x-axis – the longitudinal axis – directed from the aft to the bow, y-axis – the transverse axis – directed from port to starboard, and z-axis – the normal axis – directed from top to bottom [Skjetne, 2005].

The vectors $\boldsymbol{\eta}$ and $\boldsymbol{\nu}$ define the vessel's earth-fixed position and orientation, and the body fixed translation and rotation velocities. According to SNAME [1950] these vectors can be written

$$\boldsymbol{\eta} = [x, y, z, \phi, \theta, \psi]^\top \tag{6.1}$$

$$\boldsymbol{\nu} = [u, v, w, p, q, r]^\top \tag{6.2}$$

where $\boldsymbol{\eta}$ denotes the position and orientation vector where x, y, and z is the distance from NED to BODY expressed in NED coordinates, and ϕ, θ, and ψ is a vector of Euler angles. $\boldsymbol{\nu}$ denotes the linear and angular velocity vectors which are decomposed in the body-fixed reference frame [Fossen, 2010].

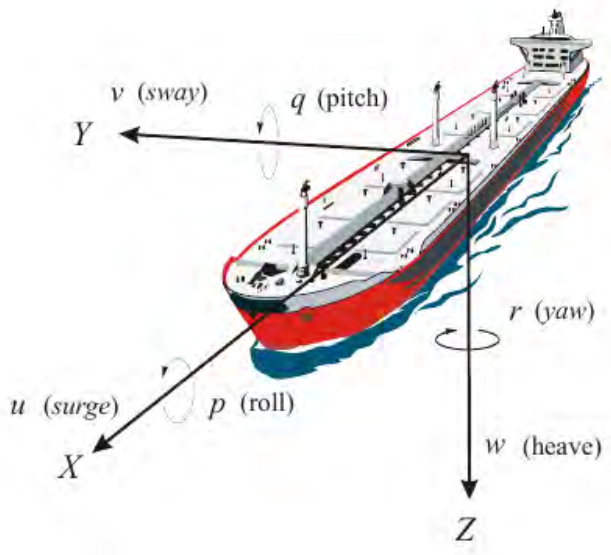

Figure 6.2: Definitions of surge, sway, heave, roll, pitch, and yaw. [Courtesy: Fossen, 2010]

Table 6.1: SNAME (1950) notation for marine vessels

DOF		forces and moments	linear and angular velocities	positions and Euler angles
1	motions in the x-direction (surge)	X	u	x
2	motions in the y-direction (sway)	Y	v	y
3	motions in the Z-direction (heave)	Z	w	z
4	rotation about the x-axis (roll)	K	p	ϕ
5	rotation about the y-axis (pitch)	M	q	θ
6	rotation about the z-axis (yaw)	N	r	ψ

6.2 Vessel Dynamics

In mathematical modeling of the marine vessel dynamics it is common to separate the total model into a Low Frequency (LF) model and a Wave Frequency (WF) model by superposition. Hence, the total motion is a sum of the corresponding LF and WF components, see Figure 6.3. The WF motions are assumed to be caused by first-order wave loads, Assuming small amplitudes these motions will be well represented by a linear model. The LF motions are assumed to be cause by second-order mean and slowly varying wave loads, current loads, wind loads, mooring and thrust forces. These motions are generally nonlinear, but linear approximations about certain operation points can be found [Sørensen, 2005].

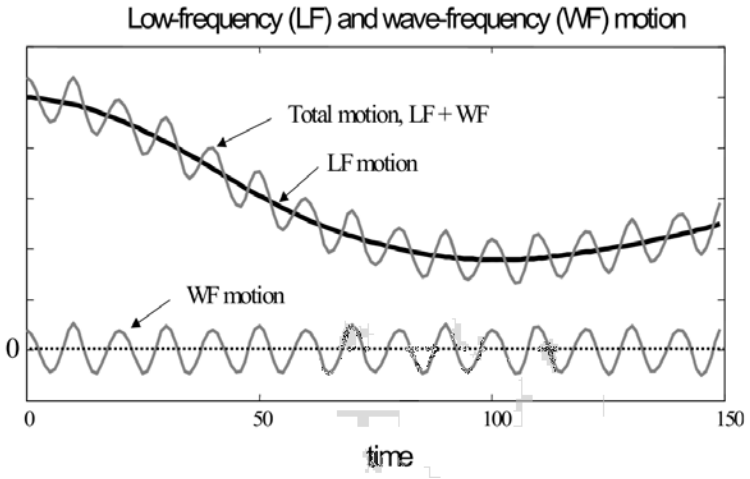

Figure 6.3: The total motion of a vessel is the sum of the WF and LF motions. [Courtesy: Sørensen, 2005]

6.3 General model

The governing frequency-independent model for marine vessels is according to [Fossen, 2010]

$$\boldsymbol{M}\dot{\boldsymbol{\nu}} + \boldsymbol{C}(\boldsymbol{\nu})\boldsymbol{\nu} + \boldsymbol{D}(\boldsymbol{\nu})\boldsymbol{\nu} + \boldsymbol{g}(\boldsymbol{\eta}) + \boldsymbol{g}_0 = \boldsymbol{\tau} + \boldsymbol{\tau}_{wind} + \boldsymbol{\tau}_{wave} \tag{6.3}$$

where

$\boldsymbol{M} = \boldsymbol{M}_{RB} + \boldsymbol{M}_A$	- system inertia matrix and added mass matrix
$\boldsymbol{C}(\boldsymbol{\nu}) = \boldsymbol{C}_{RB}(\boldsymbol{\nu}) + \boldsymbol{C}_A(\boldsymbol{\nu})$	-Coriolis-centripetal matrix (including added mass)
$\boldsymbol{D}(\boldsymbol{\nu})$	-damping matrix
$\boldsymbol{g}(\boldsymbol{\eta})$	-vector of gravitational/buoyancy forces and moments
$\boldsymbol{g}_0$	-vector for pretrimming (ballast control)
$\boldsymbol{\tau}$	-vector of control inputs
$\boldsymbol{\tau}_{wind}$	-vector of wind loads
$\boldsymbol{\tau}_{wave}$	-vector of wave loads

6.4 Nonlinear DP model

The 6DOF model described above can be simplified to a 3DOF model representation for surface vessels. This is based on the assumption that ϕ and θ are small, which is a good approximation for most conventional ships and rigs [Fossen, 2010]. Hence the vectors $\boldsymbol{\eta}$ and $\boldsymbol{\nu}$ can be rewritten to comply with the 3DOF notation.

$$\boldsymbol{\eta} = [x, y, \psi]^\top \tag{6.4}$$

$$\boldsymbol{\nu} = [u, v, r]^\top \tag{6.5}$$

The simplified 3DOF representation will be used to model CSE1 in this thesis. [Sørensen, 2005] suggests the following model as a control model for a DP vessel.

$$\dot{\boldsymbol{\eta}} = \boldsymbol{R}(\psi)\boldsymbol{\nu} \tag{6.6}$$

$$\boldsymbol{M}\dot{\boldsymbol{\nu}} + \boldsymbol{D}\nu = \boldsymbol{\tau} + \boldsymbol{R}^\top(\psi)\boldsymbol{b} \tag{6.7}$$

where $\boldsymbol{\eta}$ and $\boldsymbol{\nu}$ is given by equation 6.4 and 6.5, $\boldsymbol{b}$ is the bias vector, and $\boldsymbol{\tau} = [\tau_x, \tau_y, \tau_\psi]^\top$ is the control input vector. And $\boldsymbol{R}(\psi)$ is the rotation matrix given by equation 6.8.

$$\boldsymbol{R}(\psi) = \begin{bmatrix} \cos(\psi) & -\sin(\psi) & 0 \\ \sin(\psi) & \cos(\psi) & 0 \\ 0 & 0 & 1 \end{bmatrix} \tag{6.8}$$

For low-speed applications, the different matrices are defined according to [Sørensen, 2005]

$$\mathbf{M} = \begin{bmatrix} m - X_{\dot{u}} & 0 & 0 \\ 0 & m - Y_{\dot{v}} & mx_G - Y_{\dot{r}} \\ 0 & mx_G - N_{\dot{v}} & I_z - N_{\dot{r}} \end{bmatrix} \tag{6.9}$$

$$\mathbf{D} = \begin{bmatrix} -X_u & 0 & 0 \\ 0 & -Y_v & -Y_r \\ 0 & -N_v & -N_r \end{bmatrix} \tag{6.10}$$

where $\boldsymbol{M}$ is the mass matrix, consisting of the rigid body mass and added mass, and $\boldsymbol{D}$ is the linear damping mass. In the general case, both the added mass and damping are considered to be frequency dependent, but in this case under the assumption of low speed, and no waves, both the added mass and damping are considered constant.

6.5 Control Allocation

For marine crafts in n DOF it is necessary to distribute the generalized control forces $\boldsymbol{\tau} \in \mathbb{R}^n$ to the actuators in terms of control inputs $\boldsymbol{u} \in \mathbb{R}^r$ as shown in Figure 6.4. If $r > n$ this is an over-actuated control problem, while $r < n$ is referred to as an under-actuated control problem [Fossen, 2010].

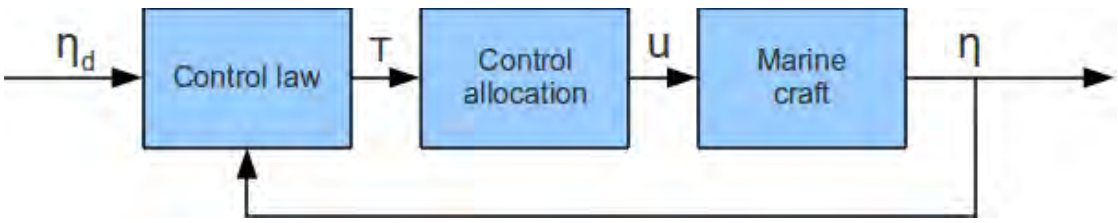

Figure 6.4: Block diagram showing the control allocation block in a feedback control system. Adapted from [Fossen, 2010].

The calculation of u from $\boldsymbol{\tau}$ is a model-based optimization problem. The solutions to this problem can range from the simplest where rate constrains on the thrusters is unaccounted for and for instance rotatable thrusters are allowed to rotate in any given direction. The more sophisticated control allocation solutions take into account these factors, to avoid instances where for example the wake from a azipod is directed onto another propeller.

To create a control allocation, a model of the vessels actuators is needed. The simplest model (linear) can be written

$$F = ku \tag{6.11}$$

where F is the generated force, k is the force coefficient, and u is the control input for the actuator. With this model it is simple to calculate the control input u when the desired force and force coefficient is known.

When solving the control allocation problem, one can decompose the force from rotatable thruster (the VSPs in this case) into two force components. In Figure 6.5 this is shown, where the port VSP can generate the two force components F_{x1} and F_{y1}, and the starboard VSP can generate the two force components F_{x2} and F_{y2}. The bow thruster can only generate thrust sideways and has therefore only one force component F_{x3}.

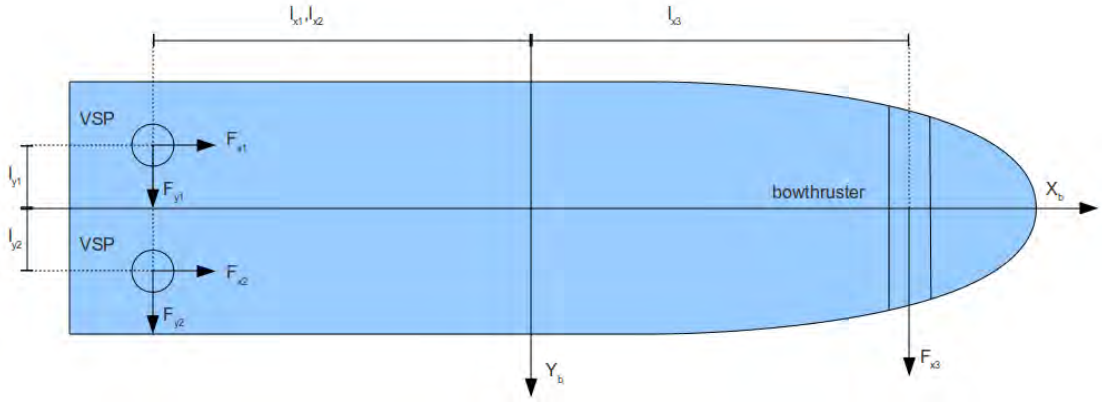

Figure 6.5: Schematic drawing of the thruster configuration for CSE1

With this assumption one can derive the extended thrust matrix for CSE1. The equation for the extended thrust matrix yields

$$\boldsymbol{\tau}_e = \boldsymbol{T}_e \boldsymbol{K}_e \boldsymbol{u}_e \tag{6.12}$$

$$\begin{bmatrix} X \\ Y \\ N \end{bmatrix} = \begin{bmatrix} 1 & 0 & 1 & 0 & 0 \\ 0 & 1 & 0 & 1 & 1 \\ l_{y1} & -l_{x1} & -l_{y2} & -l_{x2} & l_{x3} \end{bmatrix} \begin{bmatrix} K_1 & 0 & 0 & 0 & 0 \\ 0 & K_2 & 0 & 0 & 0 \\ 0 & 0 & K_3 & 0 & 0 \\ 0 & 0 & 0 & K_4 & 0 \\ 0 & 0 & 0 & 0 & K_5 \end{bmatrix} \begin{bmatrix} u_1 \\ u_2 \\ u_3 \\ u_4 \\ u_5 \end{bmatrix} \tag{6.13}$$

where $\boldsymbol{T}_e$ is the thrust configuration matrix, $\boldsymbol{K}_e$ is a gain matrix, and $\boldsymbol{u}_e$ is the control input vector with $F_{x1} = K_1 u_1$, $F_{y1} = K_2 u_2$, $F_{x2} = K_3 u_3$, $F_{y2} = K_4 u_4$, and $F_{y3} = K_5 u_5$. The control input u is normalized such that $|u| = 1$ gives $F = F_{max}$.

Equation 6.13 is derived by summing the force vectors from all the thruster components. For component u_1, the resulting thrust vector would be

$$\boldsymbol{\tau_1} = \begin{bmatrix} X_1 \\ Y_1 \\ N_1 \end{bmatrix} = \begin{bmatrix} K_1 u_1 \\ 0 \\ l_{y1} K_1 u_1 \end{bmatrix} \tag{6.14}$$

For the VSPs the relation between the two force component is restricted such that

$$\sqrt{u_1^2 + u_2^2} \leq F_{max} \tag{6.15}$$

6.6 Wave spectrum

When CSE1 will be tested in the presence of irregular waves, the Joint North Sea Wave Project (JONSWAP) spectra will be used for calculation of the wave elevation generated by the wave maker in the MC Lab. The JONSWAP spectra has the following spectrum function [Faltinsen, 1990]

$$S(\omega) = 155 \frac{H_{\frac{1}{3}}^2}{T_1^4 \omega^5} \exp\left(\frac{-944}{T_1^4 \omega^4}\right)(3.3)^Y \tag{6.16}$$

where

$$Y = \exp\left(-\left(\frac{0.191\omega T_1 - 1}{2^{\frac{1}{2}}\sigma}\right)^2\right) \tag{6.17}$$

and

$$\sigma = \begin{cases} 0.07 & \text{for } \omega \leq \frac{5.24}{T_1} \\ 0.09 & \text{for } \omega > \frac{5.24}{T_1} \end{cases} \tag{6.18}$$

and T_1 is the mean wave period, and $H_{\frac{1}{3}}$ is the significant wave height defined as the mean of the one third highest waves.

Chapter 7

System identification

Now that the models that will be used are established, it is time to focus on the parameter estimation. As we will see later, the controller design is based on the vessels dynamics. So in order to achieve good performance of the control system, it is necessary to have a proper mathematical model of the vessel. An accurate mathematical model is important for the controller design, and can also be used for a HIL simulator.

There exists several different approaches for obtaining a ship's parameters, both numerical and experimental depending on the parameters of interest. For full scale ships, parameter estimation is done numerically during the design process, and often verified by full scale tests after commissioning. For full scale ships, for instance, added mass and damping are calculated by the use of software that uses for instance strip theory or potential theory. These calculations are based on the vessels geometry. Todays "industry standard" hydrodynamical SW programs such as *Wadam, Wasim, Vres* and *Wamit* computes both frequency dependent added mass and frequency dependent damping.

Even though advanced hydrodynamical SW is available, several tests are often preferred executed in full scale. For instance "bollard pull" tests are done on a lot of vessels before they enter service. The "bollard pull" test is a test where the vessel is moored to a mooring bollard onshore, and commands full thrust to measure the maximum pulling force of the vessel. Other types of tests include free running tests such as "Zig-Zag" maneuver, "crash stop" maneuver, and "turning circle" maneuver [Faltinsen, 2005]. These tests are used for identification of "high speed" parameters, that is in the area of interest when dealing with for instance autopilots, and are therefore not in the scope of this thesis.

Model tests are widely used to verify design of new vessels. If an experiment from a model test reveals that a parameter is not as expected, it is favorable to detect this as early as possible before the building of the full scale ship has started.

For the parameter identification of CSE1 towing tests and bollard pull tests were con-

ducted. These tests can only provide some of the vessels parameters of interest, and therefore the rest of the parameters were attempted to identify by use of the System Identification ToolBox (SITB). The input data that was analyzed with SITB is recorded from free running tests.

7.1 Surge and sway damping

The surge damping coefficient can be found by towing CSE1 at constant speeds, and then measure the towing force (drag force). Equation 6.7 on page 45 is used to derive the expression used for the surge damping. Assuming that the towing is conducted at constant speed, the acceleration is zero, and hence the $\boldsymbol{M}\dot{\boldsymbol{\nu}}$ term is zero. It is also assumed that there is no bias, such that the $\boldsymbol{R}^{\top}(\psi)\boldsymbol{b}$ term is also zero. When solving for the damping matrix, one gets

$$\boldsymbol{D} = \frac{\boldsymbol{\tau}}{\boldsymbol{\nu}} \tag{7.1}$$

Considering only the surge direction and rearranging the equation, one gets

$$X_u = -\frac{\tau_x}{u} \tag{7.2}$$

In order to measure the towing forces, two force rings (strain gauges) are applied. One attached in the bow, and one in the stern, see Figure 7.1. After the force ring in the stern, a spring is placed, to ensure a minimum tension on the lines. The tension in the lines ensures that the ship is directional stable when towed. Before any towing and measurements are performed, the force rings are calibrated, and the zero point is adjusted such that zero force readings is obtained when the towing lines are tightened, and the vessel is at rest. The towing cables are attached to the towing carriage. The towing carriage was driven at several different speeds, in both forward and backward direction for a period of $30 - 40$ seconds. The force measurements were started some seconds after the towing carriage had reached the target speed for each run, in order to not measure when there is accelerations involved.

Figure 7.1: Schematic of the setup used to measure sway damping and force from the VSPs in the sway direction.

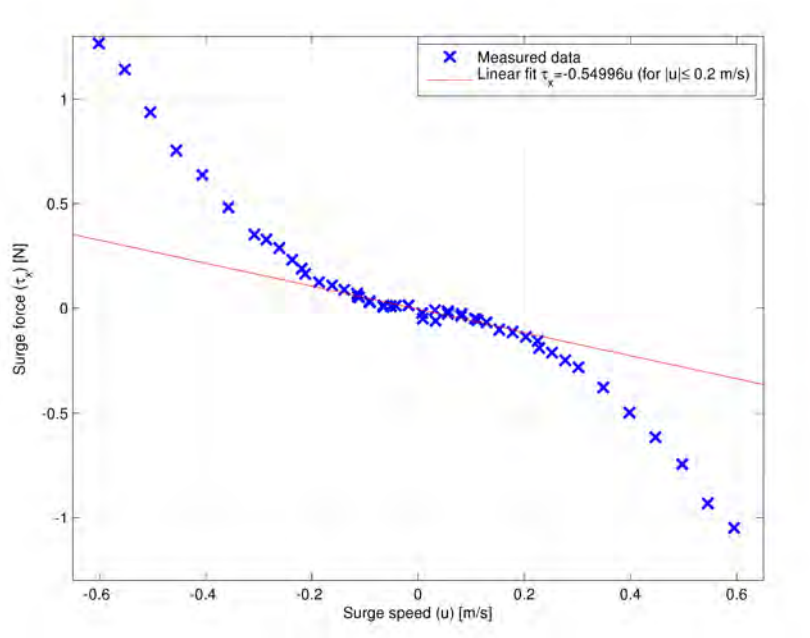

Figure 7.2: Measured drag forces for CSE1 at different speeds, and corresponding linear fit for the damping coefficient in the range $|u| \leq 0.2\ m/s$. The linear surge damping $X_u \approx -0.55\ kg/s$.

To find the sway damping, the same approach as for surge is applied. The major difference being that four towing lines and force rings are applied in stead of two. See Figure 7.3.

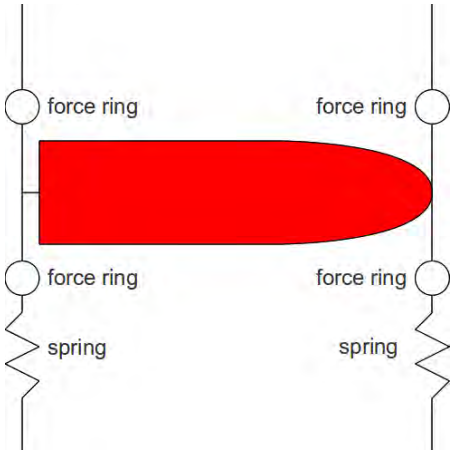

Figure 7.3: Schematic of the setup used to measure surge damping and force from the VSP in the surge direction

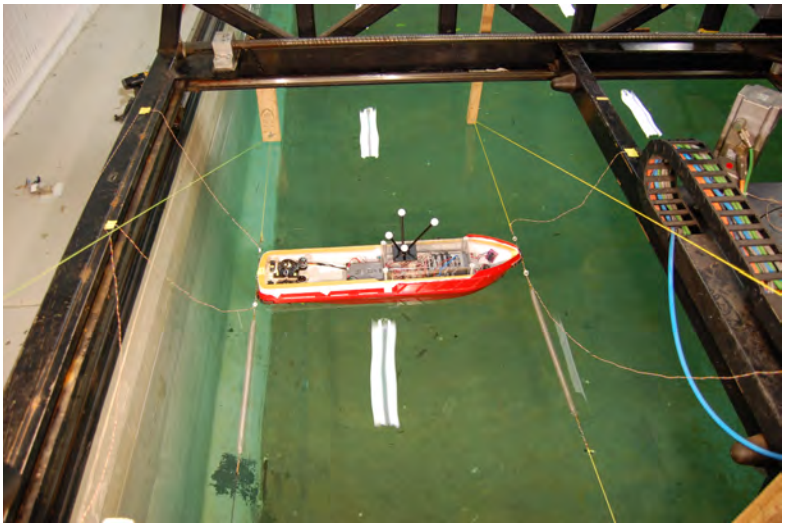

Figure 7.4: Photograph of the setup used to measure drag forces in sway.

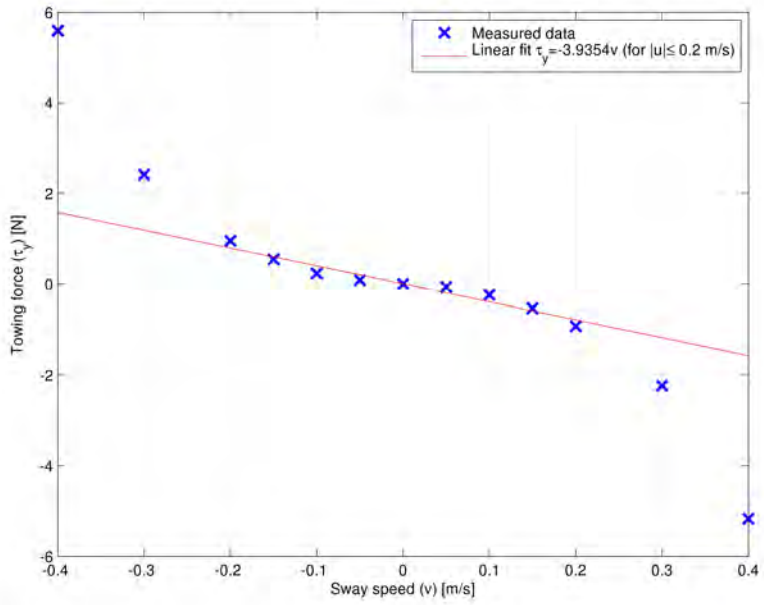

Figure 7.5: Measured drag forces for CSE1 at different speeds, and corresponding linear fit for the damping coefficient in the range $|u| \leq 0.2m/s$. The linear sway damping $Y_v \approx -3.94kg/s$

In Figure 7.5 and 7.2 on the preceding page one can clearly see that the damping is linear for low speeds and that the damping rapidly increases for higher speeds.

Yaw damping could in theory also be determined by the same methods as applied for surge and sway. However, the MC Lab lacks equipment for rotating a vessel with constant rotational velocity, and simultaneously measuring the moment.

7.2 Thruster force coefficients

The thrust magnitude from the VSPs is determined by both its rotational speed, and the blade pitch. From the experiments with manual control it was found out that setting the rotational speed set-point to 40% of maximum, provided a maximum thrust more realistic to the vessel. Therefore the rotational speed set-points for the VSPs will be set to 40% for DP and joystick mode. This is also done to reduce the number of control inputs, and thereby make a simpler system. All the results presented for in this section are measured with the rotational speed at 40%. A more sophisticated DP system should take into account that the power from the VSP is also a matter of the rotational speed, and hence control this parameter as well. Controlling both the rotational speed and the blade pitching would allow for a more economical (fuel efficient) DP system.

To measure the force from the actuators on CSE1, the same setup as used for surge and sway damping were used. This time all the measurements were conducted with zero speed. These measurements were done to gain knowledge about the maximum thrust from the different actuators, as well as creating a mapping for the thruster set-points. Because the force from the VSPs is decomposed into two force components (for the thrust configuration matrix), the thrust is treated as two components, and measured separately. One could assume that the VSPs are able to produce an equal amount of thrust in all directions, and its set-points for the same amount of thrust wold be the same. This assumption is believed to be valid for the VSP alone, due to its symmetry. However, due to hydrodynamical interaction with the hull, and interaction between the two VSPs, it is desirable to measure the generated thrust in both positive and negative for each force component separately.

To map the thrust from the VSPs, three different models were suggested

$$F = kp \tag{7.3}$$

$$F = k|p|p \tag{7.4}$$

$$F = k_1|p|p + k_2 p \tag{7.5}$$

where F is the measured force, k is the force coefficient(s) and p is the relative pitch $-1 \leq p \leq 1$.

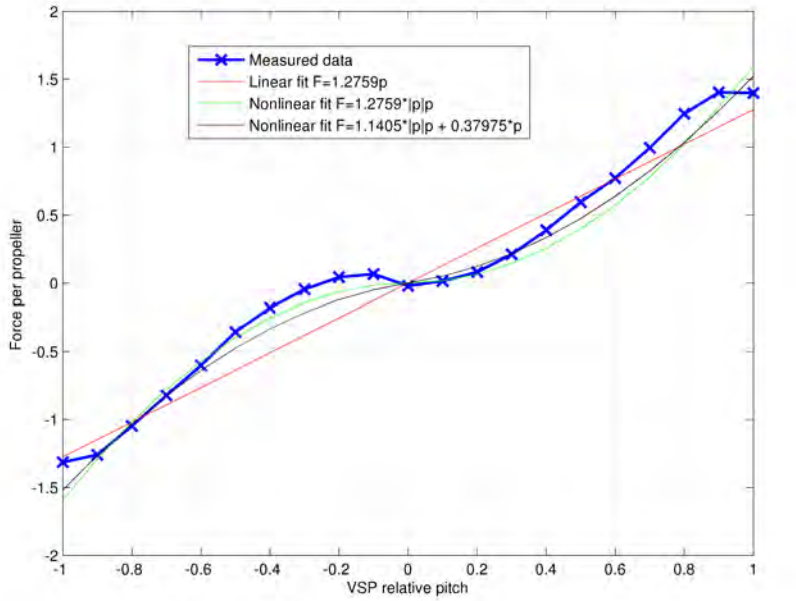

Figure 7.6: Measured thrust per VSP in surge direction.

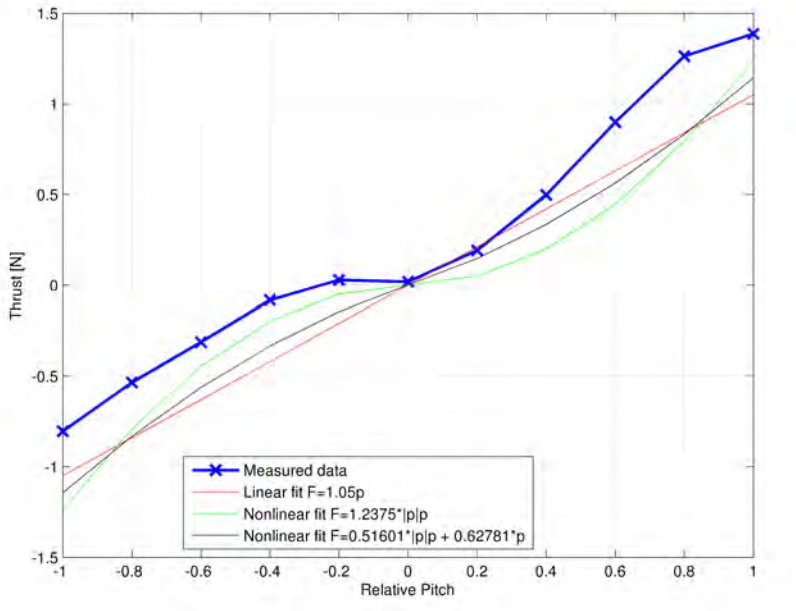

Figure 7.7: Measured thrust from the port VSP in sway direction

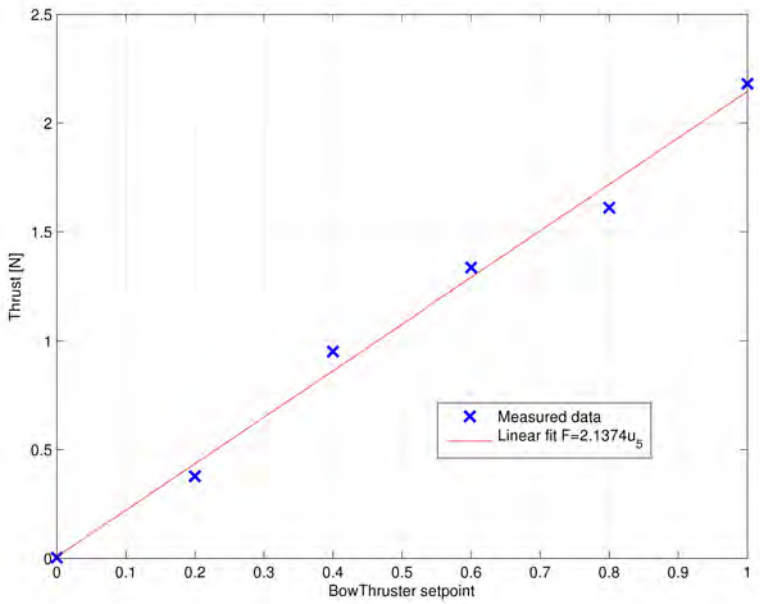

Figure 7.8: Measured thrust from the bow thruster versus bow thruster set-points.

Some comments to Figure 7.6 on the preceding page and 7.7 on the facing page are needed. First of all it is observed that none of the suggested thruster models fit really well. And it is hard to decide by visual inspections which model fits the best to the measured data. However, the linear model will be used due to its simplicity of implementation. For both the mentioned figures, it is clear that the assumption that the generated thrust will not be "symmetric", i.e. that $F(p) \neq F(-p)$ seems to be valid. It is also somehow surprising that the force is positive for $p = -0.2$ in both cases. This might relate to the propeller rake being directed backwards when it hits the hull or the other VSP (for sway), and thereby creating a force in the opposite direction of what one could expect. Another possibility is that these readings are related to measurement errors.

From Figure 7.8 one can see that the linear model fits a lot better than for the VSPs. To model the bow thruster according to a linear thruster model is a decent assumption.

7.3 Added mass estimation

As mentioned before, the added mass is normally calculated using hydrodynamical SW based on the geometry of the hull. Because we do not possess any 3D drawing of the vessel, such methods can not be used. However, there exist some other estimation

formulas for added mass. [Lewandowski, 2004] suggests a method named "equivalent ellipsoid" for added mass estimation of ships. This method calculates the added mass based on an assumption that the hull has a shape of a spheroid with corresponding waterline length, draft, or beam. The formulas for this added mass estimation are given below

$$A_{11} = -X_{\dot{u}} = -\rho\nabla\kappa_1 \tag{7.6}$$

$$A_{22} = -Y_{\dot{v}} = -\rho\nabla\kappa_2 \tag{7.7}$$

where, κ_1 and κ_1 are given as

$$\kappa_1 = \frac{\alpha_0}{2-\alpha_0} \tag{7.8}$$

$$\kappa_2 = \frac{\beta_0}{2-\beta_0} \tag{7.9}$$

where

$$\alpha_0 = \frac{2(1-e^2)}{e^3}[\frac{1}{2}\ln(\frac{1+e}{1-e}) - 1] \tag{7.10}$$

$$\beta_0 = \frac{1}{e^2} - \frac{1-e^2}{2e^3}\ln(\frac{1+e}{1-e}) \tag{7.11}$$

and

$$e = \sqrt{1-\frac{d^2}{L^2}} \tag{7.12}$$

where d and L are the maximum diameter and length overall. Solving these equations with the data from CSE1 gives $X_{\dot{u}} = -0.35\ kg$ and $Y_{\dot{v}} = -13.4\ kg$. These numbers are only estimates, of the added mass, and will therefore be used as an initial guess for the parameter estimation presented in the next section.

7.4 Parameter estimation using Matlab

The methods presented above will only provide some of the parameters to Equation 6.7 on page 45. An objective of this thesis is to investigate if Matlab's SITB can be used for parameter estimation in a marine control context. The idea is to record data-series of the input to CSE1 (thruster set-points), and output (position and orientation), and then feed this data to a grey-box model in SITB. Grey-box modeling means that an unknown process is assumed to have some given model, where the parameters are unknown. This differs to black-box modeling where both the model and its parameters are assumed unknown. In this case the model for our grey-box will be Equation 6.7 on page 45.

In order to use this model in SITB, it needs to be rewritten into a state-space form

$$\dot{\boldsymbol{x}} = \boldsymbol{A}\boldsymbol{x}(t) + \boldsymbol{B}\boldsymbol{u}(t) \tag{7.13}$$

$$\boldsymbol{y} = \boldsymbol{C}\boldsymbol{x}(t) + \boldsymbol{D}\boldsymbol{u}(t) \tag{7.14}$$

The state vector $\boldsymbol{x}$ is set to

$$\boldsymbol{x} = \begin{bmatrix} \boldsymbol{\eta} \\ \boldsymbol{\nu} \end{bmatrix} \tag{7.15}$$

and $\boldsymbol{u} = \boldsymbol{\tau} = \boldsymbol{T}_e \boldsymbol{K}_e \boldsymbol{u}_e$ such that our state-space representation reads

$$\begin{bmatrix} \dot{\boldsymbol{\eta}} \\ \dot{\boldsymbol{\nu}} \end{bmatrix} = \begin{bmatrix} \boldsymbol{0}_{3\times3} & \boldsymbol{R}(\psi) \\ \boldsymbol{0}_{3\times3} & -\boldsymbol{M}^{-1}\boldsymbol{D} \end{bmatrix} \begin{bmatrix} \boldsymbol{\eta} \\ \boldsymbol{\nu} \end{bmatrix} + \begin{bmatrix} \boldsymbol{0}_{3\times3} \\ -\boldsymbol{M}^{-1} \end{bmatrix} \boldsymbol{\tau} + \begin{bmatrix} \boldsymbol{0}_{3\times3} \\ \boldsymbol{M}^{-1}\boldsymbol{R}^{\top}(\psi)\boldsymbol{b} \end{bmatrix} \tag{7.16}$$

$$\boldsymbol{y} = \begin{bmatrix} \boldsymbol{I}_{3\times3} & \boldsymbol{I}_{3\times3} \end{bmatrix} \begin{bmatrix} \boldsymbol{\eta} \\ \boldsymbol{\nu} \end{bmatrix} \tag{7.17}$$

The grey box model is set up in Matlab using the *idnlgrey* model structure. The code for this is presented in the appendix on the attached CD-ROM. The code solves the nonlinear least-squares curve fitting problem using the *lsqnonlin* function. A total number of 5 data-series were recorded to use with SITB, and all these data-series were analyzed with different configurations of the Matlab code. Parameters that were adjusted in the Matlab code were for instance length of the data-series, initial guess for the parameters, saturations for the parameters, and number of iterations to run. Earlier experience with SITB proved that the method of estimating parameters with SITB worked for data-series generated from Simulink models, however no guarantee was given that this method would function adequately for real world data-series. Unfortunately, the parameter estimation done with SITB in this thesis did not provide the accuracy in parameter estimation as hoped for. It was found that the results from the estimation were significantly influenced by for instance the initial guess of a given parameter. The initial guesses where set by best judgment, or by estimation formulas where this was applicable. Several factors influenced the result from the estimation done with the SITB, such as selected data-series, and the duration of the data-series that were set to be analyzed.

It is estimated that the system identification code was executed over one hundred times with different configurations. One of the most accurate estimations will be presented in the sections below. Because there is really no true unique solution to the estimation, the accuracy is judged based on simulating the DP model afterwards with the obtained parameters, and comparing it to the measured data. In this estimation, the added mass estimation from Section 7.3 on page 55 was used as initial guesses. The previously estimated surge damping and sway damping where set to fixed. The length x_g was measured to be $+0.03m$. This was done by carefully balancing the model boat on a small tube, and measure the distance from midship to the tipping point once that had been established.

For simplicity all the thrusters are modeled according to $F = ku$ in this estimation. Whether this model is the best can be discussed, but previous experiments with other thruster models had shown that there is little or no improvements in the parameter estimation with the use of other thruster models. Other estimations had these parameters set to fixed, but experience had showed that setting these parameters as unknowns gives

more room for adaption. As seen in the Matlab output below, the system has a total of 26 parameters, where 18 are assumed unknown. The mass and geometry ($l_{x1}, l_{y1}, l_{x2}, l_{y2}$, and l_{x3}) is set to fixed, as one can be certain that these parameters are correct.

Because these analysis might take some time, an email notification has been implemented. The final part of the code sends an email with the text output presented, as well as the figures. The email notification will only work with *Googles Gmail* accounts.

Listing 7.1: Output of Matlab function describing the inputs states outputs and parameters of the idnlgrey model structure

```
Time-continuous nonlinear state-space model defined by 'cse1_m4' (MATLAB file):

   dx/dt = F(t, u(t), x(t), p1, ..., p26)
    y(t) = H(t, u(t), x(t), p1, ..., p26) + e(t)

with 5 inputs, 6 states, 6 outputs, and 18 free parameters (out of 26).

Inputs:
   u(1)   u1(t) [-]
   u(2)   u2(t) [-]
   u(3)   u3(t) [-]
   u(4)   u4(t) [-]
   u(5)   u5(t) [-]
States:                  initial value
   x(1)   North(t) [m]   xinit@exp1   -1.19569   (fix) in [-Inf, Inf]
   x(2)   East(t) [m]    xinit@exp1    1.83972   (fix) in [-Inf, Inf]
   x(3)   psi(t) [rad]   xinit@exp1    1.35281   (fix) in [-Inf, Inf]
   x(4)   u(t) [m/s]     xinit@exp1          0   (est) in [-Inf, Inf]
   x(5)   v(t) [m/s]     xinit@exp1          0   (est) in [-Inf, Inf]
   x(6)   r(t) [rad/s]   xinit@exp1          0   (est) in [-Inf, Inf]
Outputs:
   y(1)   North(t) [m]
   y(2)   East(t) [m]
   y(3)   Psi (Yaw)(t) [rad]
   y(4)   Surge speed(t) [m/s]
   y(5)   Sway speed(t) [m/s]
   y(6)   Yaw rate(t) [rad/s]
Parameters:            value
   p1    m [kg]          14.1   (fix) in [-Inf, Inf]
   p2    Xud [kg]        -0.6   (est) in [-5, -0.3]
   p3    Yvd [kg]         -15   (est) in [-20, -5]
   p4    Yrd [kg]        -0.1   (est) in [-50, 50]
   p5    Nvd [kg]        -0.1   (est) in [-50, 50]
   p6    Nrd [kg]        -0.7   (est) in [-50, 0]
   p7    Xu [kg/s]      -0.55   (fix) in [-2, -0.1]
   p8    Yv [kg/s]      -3.94   (fix) in [-10, -0.2]
   p9    Yr [kg/s]       -0.1   (est) in [-30, 30]
   p10   Nv [kg/s]          1   (est) in [-30, 30]
   p11   Nr [kg/s]       -0.3   (est) in [-30, 0]
   p12   xg [m]          0.03   (est) in [-0.1, 0.1]
   p13   Iz [kg*m^2]      1.4   (est) in [1, 2]
   p14   lx1 [m]         0.425   (fix) in [-Inf, Inf]
   p15   ly1 [m]         0.055   (fix) in [-Inf, Inf]
   p16   lx2 [m]         0.425   (fix) in [-Inf, Inf]
   p17   ly2 [m]         0.055   (fix) in [-Inf, Inf]
   p18   lx3 [m]         0.425   (fix) in [-Inf, Inf]
   p19   K1 [N]           1.28   (est) in [0.5, 2]
   p20   K2 [N]           1.05   (est) in [0.5, 2]
   p21   K3 [N]           1.28   (est) in [0.5, 2]
   p22   K4 [N]           1.05   (est) in [0.5, 2]
   p23   K5 [N]           2.14   (est) in [0.5, 10]
   p24   b1 [N]              0   (est) in [-10, 10]
   p25   b2 [N]              0   (est) in [-10, 10]
   p26   b3 [N]              0   (est) in [-10, 10]
```

The input data used for this simulation is presented in Figure 7.10 on the next page and Figure 7.9 on the following page.

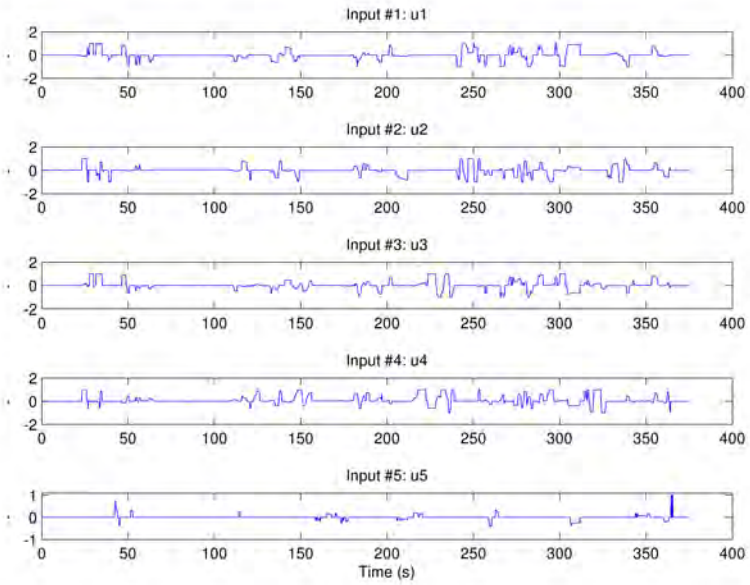

Figure 7.9: Thruster commands used for parameter estimation.

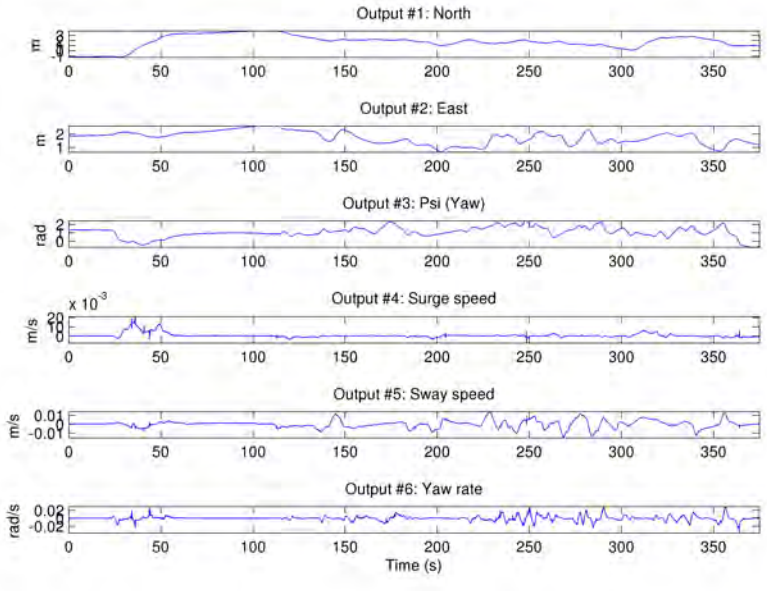

Figure 7.10: Measured states used for parameter estimation.

Listing 7.2: Output of the iteration process

```
 Criterion: Trace minimization
   Scheme: Trust-Region Reflective Newton (LSQNONLIN, LargeScale = 'On')
```

Iteration	Cost	Norm of step	First-order optimality
0	11.0663	–	–
1	11.0663	0.676	4.85e+07
2	8.23487	0.169	8.94e+07
3	6.42983	0.338	6.37e+07
4	4.53739	0.676	3.69e+07
5	2.20383	0.802	8.77e+07
6	1.80606	0.784	7.9e+07
7	1.00909	0.521	1.2e+07
8	0.938951	0.614	9.02e+06
9	0.938951	0.593	9.02e+06
10	0.827358	0.148	6.83e+06
11	0.670991	0.297	4.22e+06
12	0.657516	0.000396	1.38e+07
13	0.645866	0.000106	3.77e+06
14	0.558998	0.00279	1.57e+07
15	0.541245	0.000139	2.57e+06
16	0.46095	0.33	5.75e+06
17	0.45084	0.044	5.83e+06
18	0.441418	0.0433	5.03e+06
19	0.437042	0.0381	5.32e+06
20	0.432787	0.0376	4.78e+06
21	0.430841	0.0341	5.16e+06
22	0.429122	0.0341	4.78e+06
23	0.427319	4.37e-05	1.37e+06
24	0.421289	0.000523	5.73e+06
25	0.418693	5.46e-05	9.83e+05

```
Estimation time   : 1.57e+04 seconds
Time per iteration: 603.9 seconds.
```

Listing 7.3: Output from Matlab presenting the estimated parameters

```
Time-continuous nonlinear state-space model defined by 'cse1_m4' (MATLAB file):

   dx/dt = F(t, u(t), x(t), p1, ..., p26)
    y(t) = H(t, u(t), x(t), p1, ..., p26) + e(t)

with 5 inputs, 6 states, 6 outputs, and 18 free parameters (out of 26).

Inputs:
   u(1)    u1(t) [-]
   u(2)    u2(t) [-]
   u(3)    u3(t) [-]
   u(4)    u4(t) [-]
   u(5)    u5(t) [-]
States:                  initial value
   x(1)    North(t) [m]    xinit@exp1     -1.19569    (fix) in [-Inf, Inf]
   x(2)    East(t) [m]     xinit@exp1      1.83972    (fix) in [-Inf, Inf]
   x(3)    psi(t) [rad]    xinit@exp1      1.35281    (fix) in [-Inf, Inf]
   x(4)    u(t) [m/s]      xinit@exp1    0.0370485    (est) in [-Inf, Inf]
   x(5)    v(t) [m/s]      xinit@exp1    -0.104336    (est) in [-Inf, Inf]
   x(6)    r(t) [rad/s]    xinit@exp1      0.77713    (est) in [-Inf, Inf]
Outputs:
   y(1)    North(t) [m]
   y(2)    East(t) [m]
   y(3)    Psi (Yaw)(t) [rad]
   y(4)    Surge speed(t) [m/s]
   y(5)    Sway speed(t) [m/s]
   y(6)    Yaw rate(t) [rad/s]
Parameters:             value          standard dev
   p1     m [kg]              14.1                 0    (fix) in [-Inf, Inf]
   p2     Xud [kg]        -2.67748          0.239336    (est) in [-5, -0.3]
   p3     Yvd [kg]        -19.9938           2.31892    (est) in [-20, -5]
   p4     Yrd [kg]         0.48225           3734.23    (est) in [-50, 50]
   p5     Nvd [kg]        -6.77422            3733.9    (est) in [-50, 50]
   p6     Nrd [kg]      -7.38588e-05           526.339    (est) in [-50, 0]
   p7     Xu [kg/s]           -0.55                 0    (fix) in [-2, -0.1]
   p8     Yv [kg/s]           -3.94                 0    (fix) in [-10, -0.2]
   p9     Yr [kg/s]         1.47519         0.0804179    (est) in [-30, 30]
   p10    Nv [kg/s]        0.887797         0.0735087    (est) in [-30, 30]
   p11    Nr [kg/s]       -0.653684          0.029075    (est) in [-30, 0]
   p12    xg [m]          0.0693938           264.837    (est) in [-0.1, 0.1]
   p13    Iz [kg*m^2]       1.38877           526.337    (est) in [1, 2]
   p14    lx1 [m]             0.425                 0    (fix) in [-Inf, Inf]
   p15    ly1 [m]             0.055                 0    (fix) in [-Inf, Inf]
   p16    lx2 [m]             0.425                 0    (fix) in [-Inf, Inf]
   p17    ly2 [m]             0.055                 0    (fix) in [-Inf, Inf]
   p18    lx3 [m]             0.425                 0    (fix) in [-Inf, Inf]
   p19    K1 [N]           0.509598         0.0115061    (est) in [0.5, 2]
   p20    K2 [N]            1.00514         0.0424404    (est) in [0.5, 2]
   p21    K3 [N]           0.503294        0.00895693    (est) in [0.5, 2]
   p22    K4 [N]           0.895142         0.0393395    (est) in [0.5, 2]
   p23    K5 [N]            2.08572          0.170373    (est) in [0.5, 10]
   p24    b1 [N]           0.0132573       0.000642147    (est) in [-10, 10]
   p25    b2 [N]            0.016099       0.000931615    (est) in [-10, 10]
   p26    b3 [N]           0.0104311       0.000664367    (est) in [-10, 10]

The model was estimated from the data set 'CS Enterprise I', which
contains 7499 data samples.
Loss function 7.35595e-08 and Akaike's FPE 7.39127e-08
```

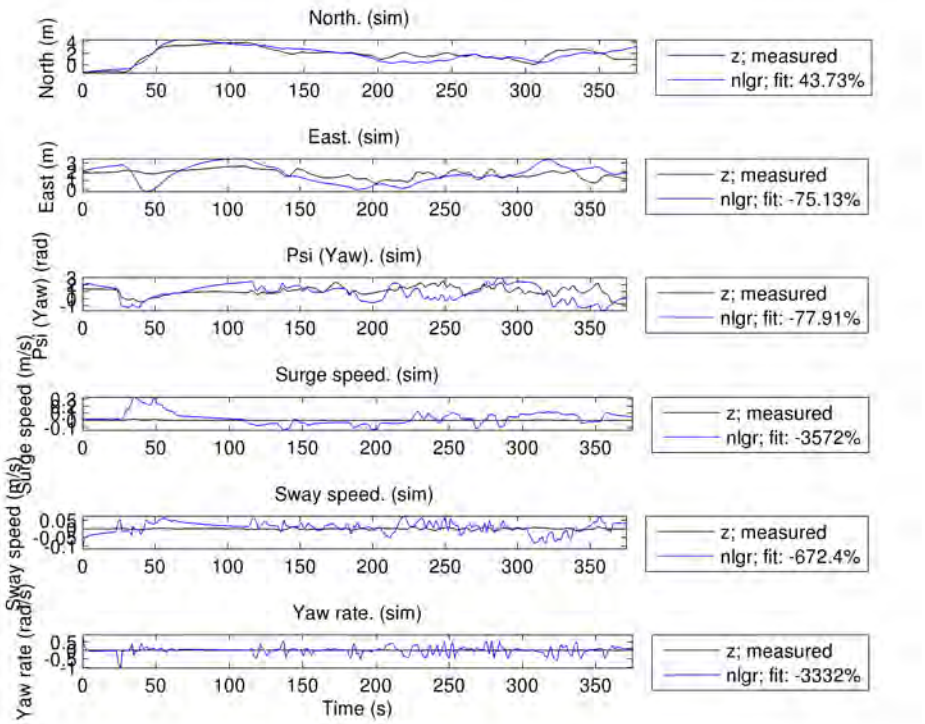

Figure 7.11: Comparison of the measured output versus the calculated output using the parameter estimates.

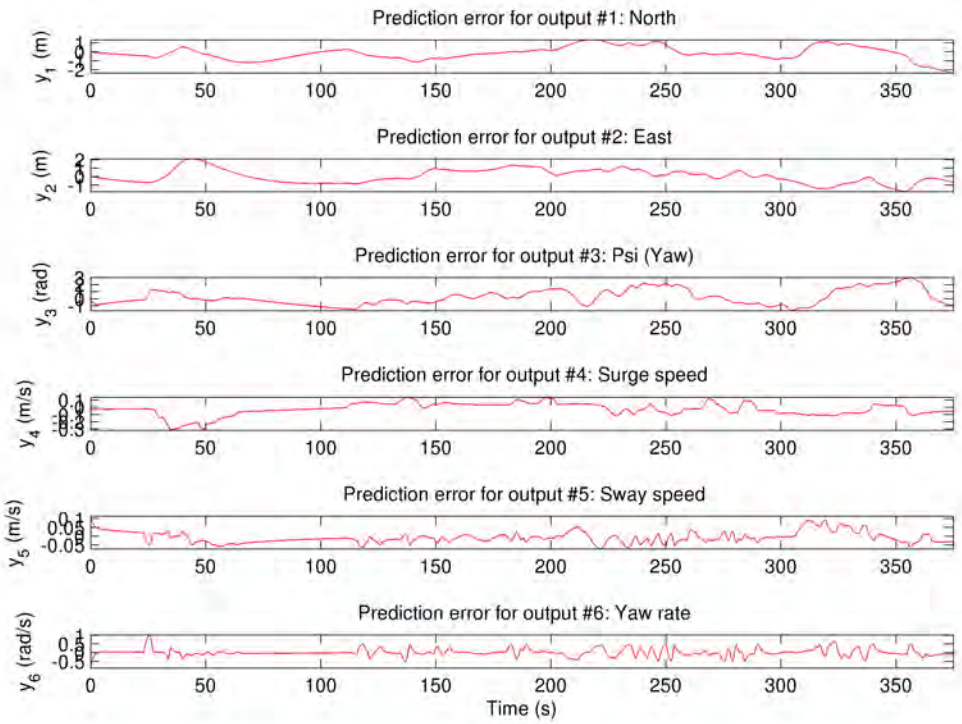

Figure 7.12: Prediction error when simulating with the obtained parameters.

Some comments to the results presented above are needed. The numerical values found for the parameter are compared to similar values found for CyberShip 2 (CS2) by [Skjetne et al., 2004]. CS2 is a model ship that is close to CSE1 in both size and geometry. The parameters are generally in the same range and magnitude, something which speaks for that the estimated values might not be that wrong after all. But what makes reasons for concern is the high standard deviation for some of the estimated values. When the estimated values have a standard deviation several times higher than the value itself, it gives low credibility to the analysis and the estimated parameters. However, the analysis is definitely "onto something". The fit for surge in Figure 7.11 on the previous page follows the contours of the measured values. If, for instance only the first 200 seconds of the same data-series are analyzed, the estimate for surge follows even better. But a smaller data-series might contain less information on the ship's dynamics, and less frequencies and other physical phenomenas might be excited.

In Figure 7.11 on the preceding page an interesting observation for yaw is done. The fit curve, and measured curve do not concur very well with each other, however at some time intervals the curves concur great in phase and magnitude, only having a close to

constant deviation. This is seen at the time intervals around 130, 240, and 330 seconds. This might indicate that some of the constants, and hence the dynamics of the estimated model is not that poor after all. The close to constant deviation might be related to some other parameter that is not estimated well.

Due to the fact that the estimated parameters will vary a lot depending on the condition of the analysis (initial guess, length of the data-series, and parameter boundaries), it was decided to reject the parameters from the analysis. Also it would be hard to decide which analysis/run the parameters should be selected from if one had to use the parameters from one of the analysis. With no parameter estimation in place, the concept of a model based controller would be hard to accomplish. Therefore it was considered that the second best option would be to use the parameters for CS2 as a basis for CSE1. This is a daring move, and definitely not best practice. However, the two ships are about the same size, and have striking similarities in hull geometry. One option that was considered was to use a mixture of parameters, i.e. use the surge damping and sway damping obtained from the towing tests, and the rest of the damping terms from CS2. However, it was considered that it would be better if all the terms were "equally wrong", rather than having a mixture of parameters. The parameters were adopted "as is", even though CS2 is slightly larger than CSE1. In hindsight one could have argued that all the parameters could be scaled, for instance linear relative to the displacement difference between the two vessels.

One should note that these decisions were made when there was only three days left of the assigned laboratory time. With the time window for the laboratory closing and a partially failed parameter estimation, desperate measures were needed to be able to demonstrate a DP system during the last laboratory days. Using the parameters for CS2 therefore seemed like the best move at the time. However, one was aware of that there was no guarantee that these parameters would work, and it should be taken into account that severe tuning of the controller might be needed.

One might ask why the SITB code did not provide any reliable parameter estimation, and there might be several reasons for this. Or maybe the right question is, how can the code/procedure be adjusted to make the parameter estimation work. After all, this way of doing parameter estimation have some advantages (like obtaining parameters that are hard to calculate numerically, or measure by experiments) if one could manage to obtain reliable parameters. Maybe the most obvious weakness of the approach presented here is that the grey-box model is the simplified LF DP model, and the data fed into the model is the total motion. The results might have been better if a model of higher fidelity was used for the estimation. Such a model should include at least Coriolis forces, and non linear damping. A more sophisticated thruster model for the VSPs would also be desirable. But the pitfall of expanding the model complexity is that one might end up having so many unknown parameters in the analyzis that the SITB analyzis will not work at all.

One might also question the validity of the simplified 3DOF model used. According to [Sørensen, 2005] and [Fossen, 2010] this model is the basis for many commercial DP systems, and questioning such an established model might be to let off a bombshell.

Another possibility why the system identification with SITB does not provide reliable results is that it might be errors in the code. There has been given great attention to track down possible errors and bugs, and the code has been tested against "perfect data" i.e. mathematical simulations with no disturbances. Even though this managed to estimate the known parameters of the "perfect data", there is no guarantee that the code is flawless.

It might also be possible that better parameter estimates could have been obtained if the surge and sway/yaw dynamics had been decoupled in the analysis, i.e. that separate analysis were created for each subsystem with different data-series as input.

Table 7.1: Model parameters for CS2 estimated by [Skjetne et al., 2004]

m	23.8	kg
I_z	1.760	$kg \cdot m^2$
x_g	0.046	m
$X_{\dot{u}}$	-2.0	kg
$Y_{\dot{v}}$	-10.0	kg
$Y_{\dot{r}}$	0	$kg \cdot m$
$N_{\dot{v}}$	0	$kg \cdot m$
$N_{\dot{r}}$	-1.0	$kg \cdot m^2$
X_u	-2.0	kg/s
Y_v	-7.0	kg/s
Y_r	-0.1	$kg \cdot m/s$
N_v	-0.1	$kg \cdot m/s$
N_r	-0.5	$kg \cdot m^2/s$

Chapter 8

Design of DP control system

This chapter will look into the DP controller design, the thrust allocation, implementation of the HIL simulator, and the GUI for the DP system.

8.1 DP controller

There are several different ways and methods to design a DP controller. Ranging from Linear Quadratic Gaussian (LQG), back-stepping, and H_∞ to list a few. However, the main objective is always to compensate for the environmental forces acting on a vessel. In this thesis, a Multiple Input Multiple Output (MIMO) nonlinear Proportional, Integral, and Derivative (PID)-controller will be designed. This controller is chosen due to its relative simplicity, and the scope of this thesis is not to come up with or design some sort of groundbreaking DP controller. The chosen DP controller is described by Fossen [2010], and neglecting the wind loads in our case the control forces $\boldsymbol{\tau}$ is set to

$$\boldsymbol{\tau} = -\boldsymbol{R}^\top(\boldsymbol{\eta})\boldsymbol{\tau}_{PID} \tag{8.1}$$

where the PID-controller is expressed in the NED frame according to

$$\boldsymbol{\tau}_{PID} = \boldsymbol{K}_p\tilde{\boldsymbol{\eta}} + \boldsymbol{K}_d\dot{\boldsymbol{\eta}} + \boldsymbol{K}_i\int_0^t \tilde{\boldsymbol{\eta}}(\tau)d\tau \tag{8.2}$$

where $\boldsymbol{K}_p$, $\boldsymbol{K}_i$, and $\boldsymbol{K}_d$ are the proportional, derivative, and integral gain matrices respectively. The controller is non linear due to the sine and cosine therms in the rotation matrix.

To determine the controller gains, Fossen [2010] suggests the following equations. A tuning constant k has been added introduced in order to be able to tune the controller

on-line.

$$\boldsymbol{K}_p = k_p \boldsymbol{M} \omega_n^2 \tag{8.3}$$
$$\boldsymbol{K}_d = k_d 2\zeta \omega_n \boldsymbol{M} \tag{8.4}$$
$$\boldsymbol{K}_i = k_i \frac{\omega_n}{10} \boldsymbol{K}_p \tag{8.5}$$

8.2 Thrust allocation

In order for the DP system to allocate the control thrust, a thrust allocation algorithm is needed. The generalized inverse method will be used.

$$\boldsymbol{u} = K_e^{-1} \boldsymbol{T}_e^{\dagger} \boldsymbol{\tau} \tag{8.6}$$

where $\boldsymbol{T}_e^{\dagger}$ denotes the pseudo inverse of the extended thrust matrix. This method does not take into account the saturation limits for the thrusters. Saturation limits were therefore implemented "outside" the thrust allocation to prevent invalid thruster commands. The method does not prevent the thrusters from generating thrust in an unwanted direction, for instance one could end up with having a VSP flush right into the other-one. This is not desirable as the thrust efficiency for both VSPs would suffer.

8.3 HIL

In Simulink, a mathematical model of the ship was created based on the modeling from chapter 6 on page 41. The input to this HIL model is the control set-points $u_1 ... u_5$, and the output is the state vectors $\boldsymbol{\eta}$ and $\boldsymbol{\nu}$. Functionality to set the states in the HIL simulator from the GUI was implemented. The parameters for the HIL model were once again adopted from CS2.

8.4 HMI

A proper GUI for the DP system is needed to gain inputs from the user, such as desired position and heading, and switch between the control modes of the vessel. The GUI for the DP system was advanced from the GUI created for manual control. Several new features were added to comply with the necessary information exchange between the human operator and the DP system. One of the challenges found during the design of the GUI is that the GUI should present all the important information to the user, but however, the user should not be overwhelmed with non essential data. Also the data should be presented in a clear and understandable manner, and the controls should be easy to use and basic functionality easily accessible.

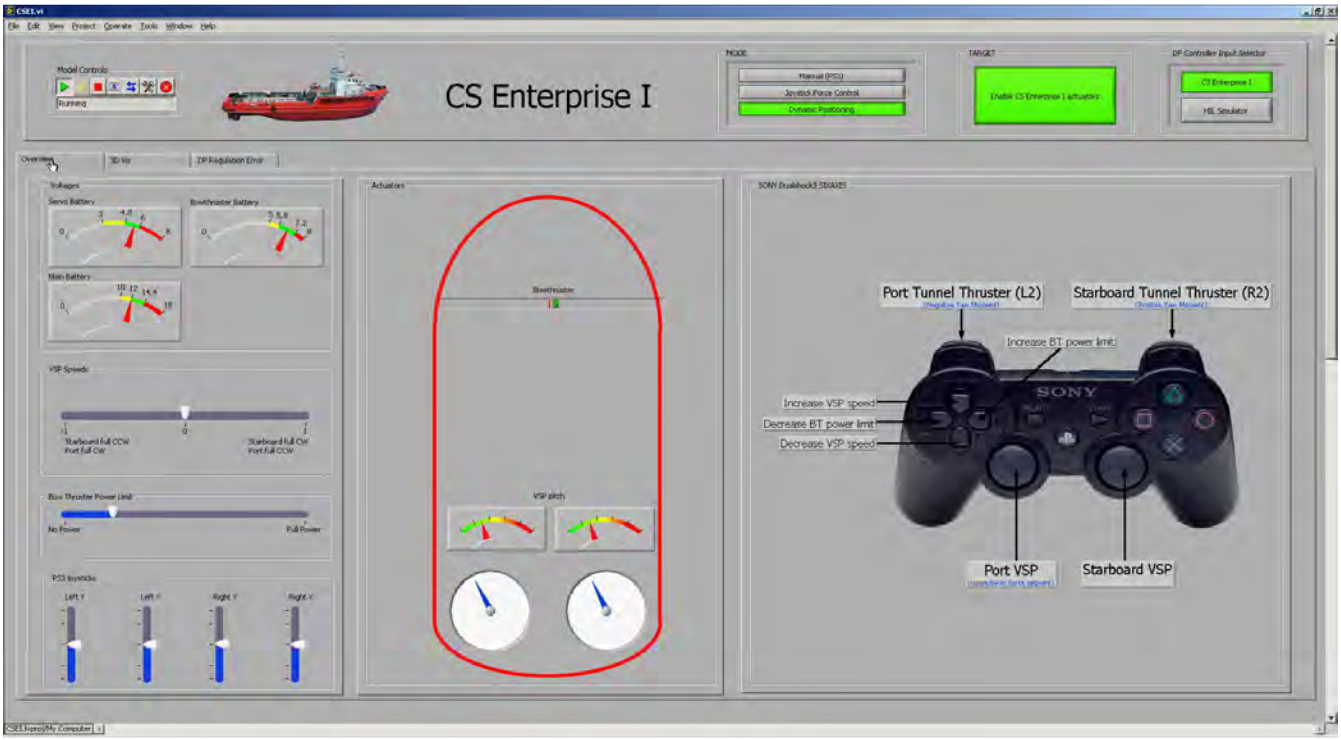

Figure 8.1: The main screen of the GUI

Figure 8.1 shows the main screen for the HMI. The controls and indicators are described below

Model Controls After the LabView program has been started, these controls controls the Compact RIO and its state. To start execution of the code loaded on the Compact RIO, press play. To stop the Compact RIO from running, press the square stop icon. To only stop the GUI from running, the round "X" button can be pressed. This action does not affect the Compact RIO state. The "Model Controls" buttons are auto generated by LabView.

Voltage shows the voltage of the three on board batteries.

VSP speeds is an indicator for the speeds of the VSPs. Only used in "manual control" mode. To set the VSPs speeds, the right and left D-pad buttons on the PS3 controller must be used.

PS3 joysticks indicates the positions of the two joysticks on the PS3 controller.

Actuators shows the state of the actuators in any operational mode for CSE1. The bow thruster set-point is indicated by a green bar proportional to the thrust set-point towards starboard, and similar a red bar for port. The blue arrows indicates

the thrust direction of the VSPs. The arrows are pointing in the wake direction. The gauges above indicates the relative pitch of the VSPs.

Sony Dualshock3 SIXAXIS describes the functions of the PS3 controller to the user, as well as indicating user actions on the PS3 controller. If a button is pressed, this is indicated by a green outline of the button. This functionality is neat to have to verify that the PS3 controller is connected properly.

Mode lets the user switch between the three operational modes of the vessel. Manual control, Joystick Force Control, and Dynamic Positioning.

Target is a switch that when enabled sends all the commands to CSE1, and enables its ESCs, and allows the actuators to operate. To only do HIL testing, i.e. no movement on the actuators of CSE1 this option should be turned off.

DP control input selector set the states to be used for the DP controller. The states can be feed from either the actual position of CSE1, or the states of the HIL simulator.

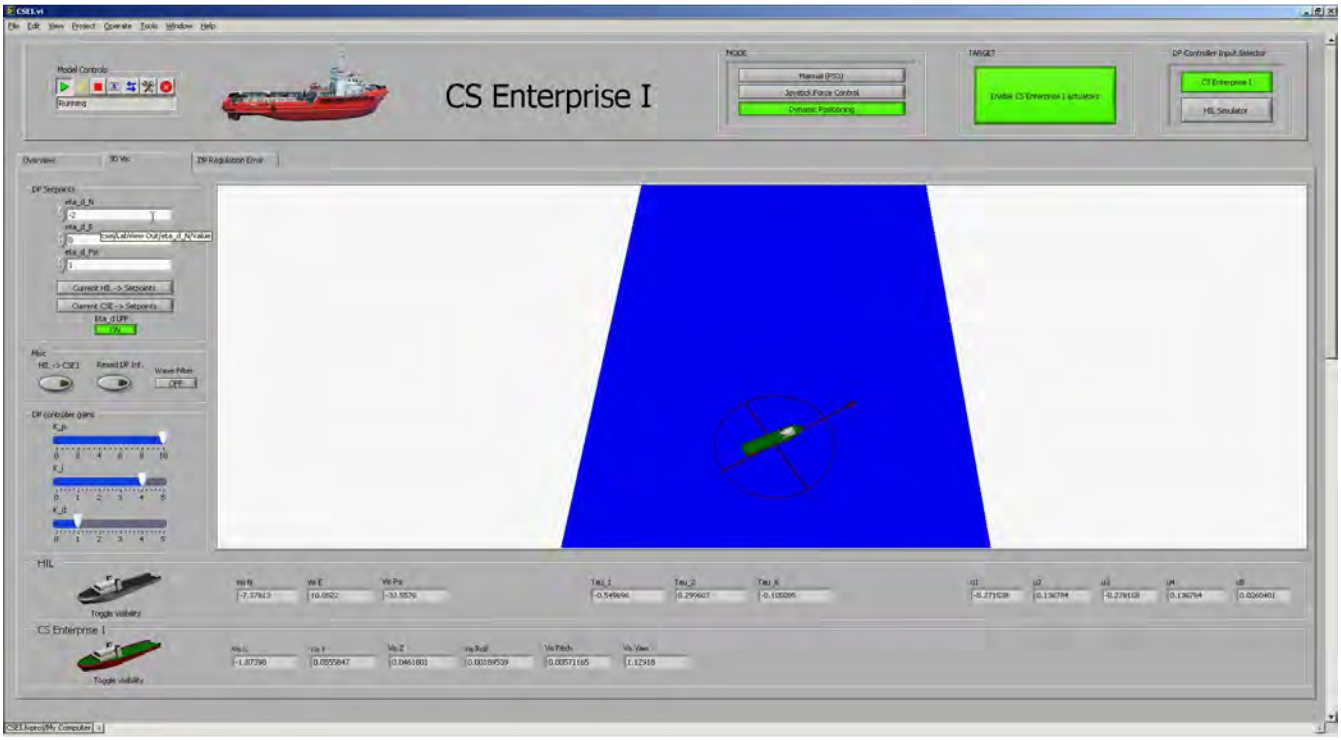

Figure 8.2: The 3D visualization screen of the GUI

Figure 8.2 shows the 3D/DP screen for the HMI. The controls and indicators are described below

DP Setpoints allows the user to manually specify the desired position and heading. Buttons for setting the desired position and heading to the current position and heading of CSE1 and the HIL simulator is below. Also a low pass filter for the desired position can be enabled.

Misc . The "HIL → CSE1" button, sets the states of the HIL model to the current states of CSE1. A button for reseting the integrator in the DP controller was implemented for testing purposes. Finally there is a button for turning on and off a planned wave filter.

DP controller gains is used to adjust the k_p, k_i, and k_d matrices in the controller. These gains can be adjusted on-line, for easier tuning of the DP controller.

HIL displays information about the HIL model to the user. By pressing the "toggle visibility" icon, the HIL model will become visible in the 3D view. The image show the HIL visibility switched off, hence the grayed out icon. The state $\boldsymbol{\eta}$, calculated thrust vector $\boldsymbol{\tau}$, and control output $\boldsymbol{u}$ is displayed by numerical indicators.

CSE1 displays the full 6DOF state vector $\boldsymbol{\eta}$ obtained from the Qualisys system. The visibility of the CSE1 can also be switched on and off in the same way as for the HIL model. The image shows the 3D model visibility set to on.

In the 3D window the approximate outline of the basin is drawn as a blue surface. To illustrate the desired position and heading for the DP system, a red arrow/circle is displayed. A red 3D model of CSE1, and a yellow 3D model are used to illustrate the position and orientation of CSE1 and the HIL model, respectively. All the 3D models are modeled in Solidworks, and exported to 3D studio MAX, and then again exported to the *.wrl* extension that the 3D functions in LabView reads. In Figure 8.3 on the following page a screen dump from 3D studio MAX in wire-frame mode is shown.

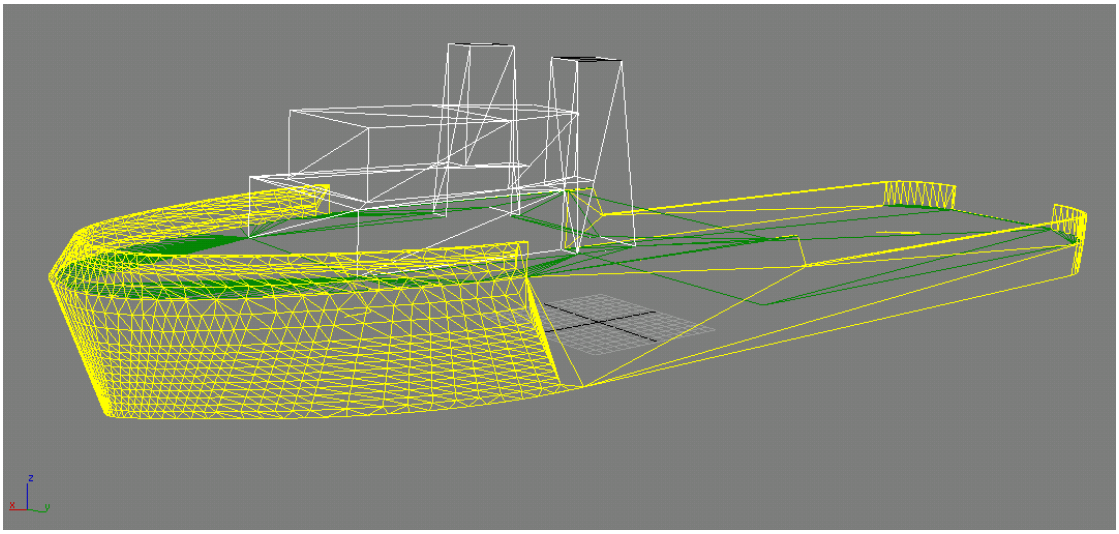

Figure 8.3: Wireframe view of the 3D visualization model

Chapter 9

HIL simulations and experiments

After the DP controller, the HMI, the HIL model, and the rest of the setup were completed, it was time for testing. The first steps were to test against the HIL model. The manual operation was first tested on the HIL simulator. This was more of a qualitative test to verify that the signal routing and so on were correctly for the manual mode, and that the HIL model behaved correct in terms of motions (i.e. verify that force towards starboard on the bow thruster gives a positive yaw rotation, and so on). This test revealed no logical or connection errors for the HIL model. As mentioned before, the HIL model were built using parameters from CS2. It was therefore expected that the response of the HIL model would differ some from the response of CSE1. The HIL model was tested in a hybrid mode versus CSE1. That is, the HIL model was tested simultaneously together with CSE1, that was on the water. The states of the HIL model were set to the states of CSE1, when CSE1 was at rest on the water. Then manual control was selected, and some arbitrary maneuvers were conducted. Then the position and orientation of CSE1 and the HIL model where compared in real-time by investigating the 3D window. This test showed that the states (position and orientation) of the HIL simulator did not follow the states of CSE1 very well for high speeds. The damping for the HIL model seemed to be to low. This accentuate the assumption made earlier that nonlinear damping should be included in the system identification as the nonlinear damping is more dominant at high speeds. For low speeds however, the difference in behavior between the HIL model and CSE1 was acceptable. Even though the dynamics of the HIL model and CSE1, had differences, the main purposes of these tests where to verify the signal routing.

After this, the joystick mode was tested. First on the HIL model. This test revealed that also the signal routing and the thrust allocation for the joystick function was working properly. The thrust allocation for joystick is the same one used for the DP system, and it is therefor important to verify that this function itself is working before testing the DP system. The HIL model behaved as desired for the joystick mode, i.e. for

instance a pure sway force set-point resulted in an almost pure sway movement (close to no yaw). However, when the joystick mode was tested for CSE1, it revealed that the joystick mode was not working properly. A commanded pure sway movement also gave a large yaw rotation. A pure surge force set-point towards starboard gave also a large positive yaw rotation (alot more thrust generated from the bow thruster than the VSPs). This indicated that the thrust coefficients found were not reliable, and possibly that the thrust coefficient for the bow thruster was underrated. At this time, a quick solution to remedy this problem was needed, as the time window for the laboratory time was once again closing fast. The quick-fix to this problem was to set $K_5 = 4.0$, i.e. almost double the estimate of the bow thruster power. The code was compiled, and joystick mode wast tested once again. This time the experience with the joystick mode was much better, the yaw induced rotation when commanding sway movement was slightly less, but yet not completely away. At least the quick-fix method worked. To further suppress the yaw rotation of a surge command, K_5 was set to 8.0. This final tweak almost completely removed the yaw rotation when sway motion was commanded. In retrospect it is believed that the origin of the unwanted yaw rotation is not due to underestimation of the bow thrusters power, but rather an overestimation of the power of the VSPs. The joystick force set-point control was tuned with very low gains, such that only small thrust forces were commanded. This resulted in that the VSPs were operating at low relative pitch. If one look into Figure 7.7 on page 54 once again, one can see that the linear approximation of the thrust versus pitch is a bad assumption for $-0.4 < p < 0$. Compared with the linear approximation of the thrust from the bow thruster, the bow thruster linear approximation is much better. This might be the source to the problems with the joystick mode in the first place.

With a quick-fix up and running for the thruster-allocation/joystick mode, it was time to test the DP controller. As earlier, the tests started out with testing on the HIL model. The result of this testing was that the vessel was able to perform station-keeping, and the regulation error converged towards zero. This result was also expected since the HIL model and DP controller where based on the same set of constants. The transmission between two position and heading set-points proved no problems either. These tests were conducted with the tunable gains k_p, k_i, and k_d all set to 1.0. The next and last phase was to test the DP system on CSE1. The initial tests focused on to obtain station-keeping in calm waters with a fixed set-point. This proved no problem for the DP system. Next, the position set-point was adjusted, and the vessel did not manage to position itself on the new set-point. CSE1 started after a while to run off uncontrolled, and the vessel was stopped switching to manual mode. With some trail and error tuning, it was found out that $k_p = 10.0$, $k_i = 4.0$, and $k_d = 1.0$ provided a much better performance. With this new configuration, the instability issues disappeared, and CSE1 was able to change to a new position and heading without problems. For the last tests, the wave maker was set to generate irregular waves using the JONSWAP wave spectra with $H_s = 0.02m$ and $T_0 = 1.2s$. The DP system performed well with waves present. CSE1 was able to obtain desired position and heading. This time it was observed tendencies to minor constant

deviations to the set-points, and once again in hindsight this might indicate that the integral constant k_i should have been set even higher. The results from this last test with waves is presented in Figure 9.1, 9.2 on the next page, and 9.3 on page 77.

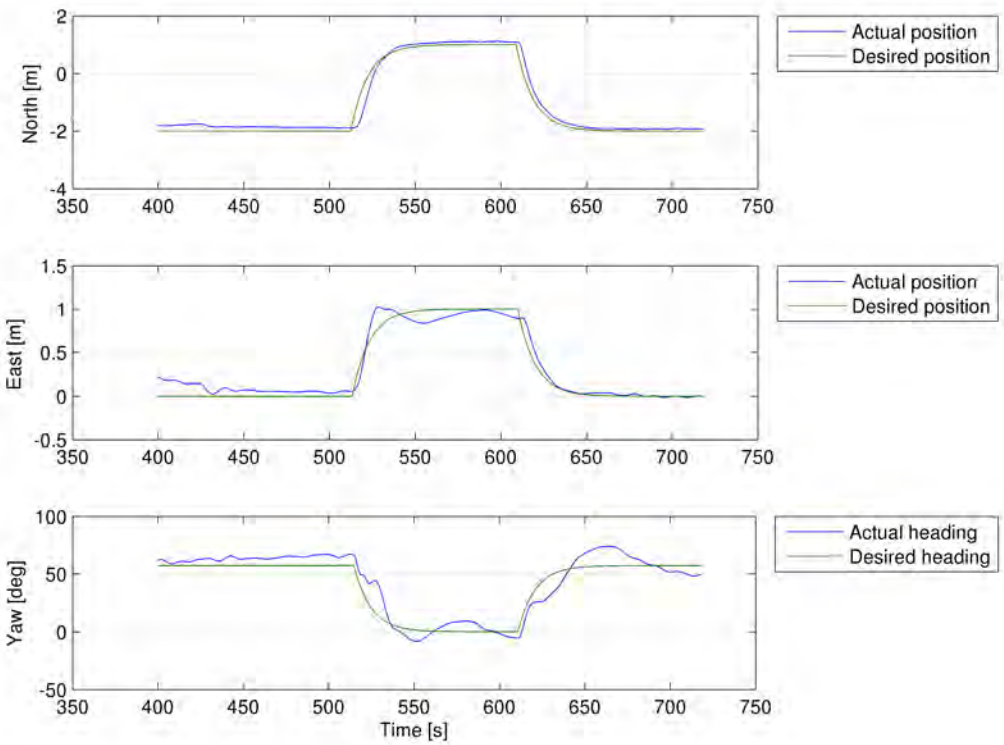

Figure 9.1: Position and heading from DP test

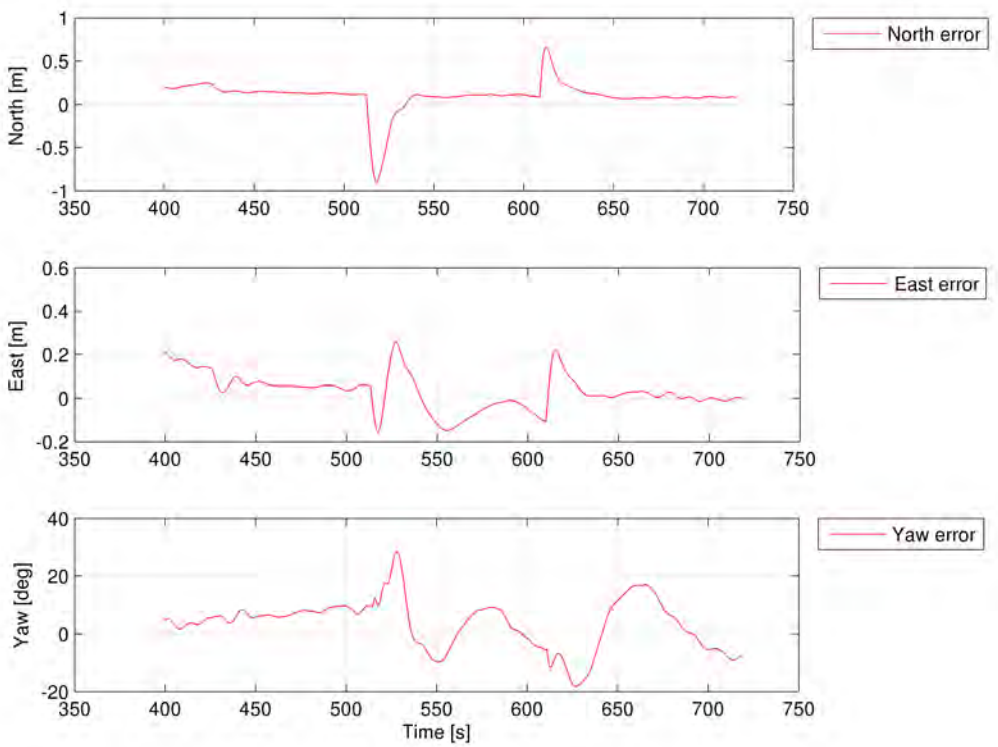

Figure 9.2: Position and heading error from DP test

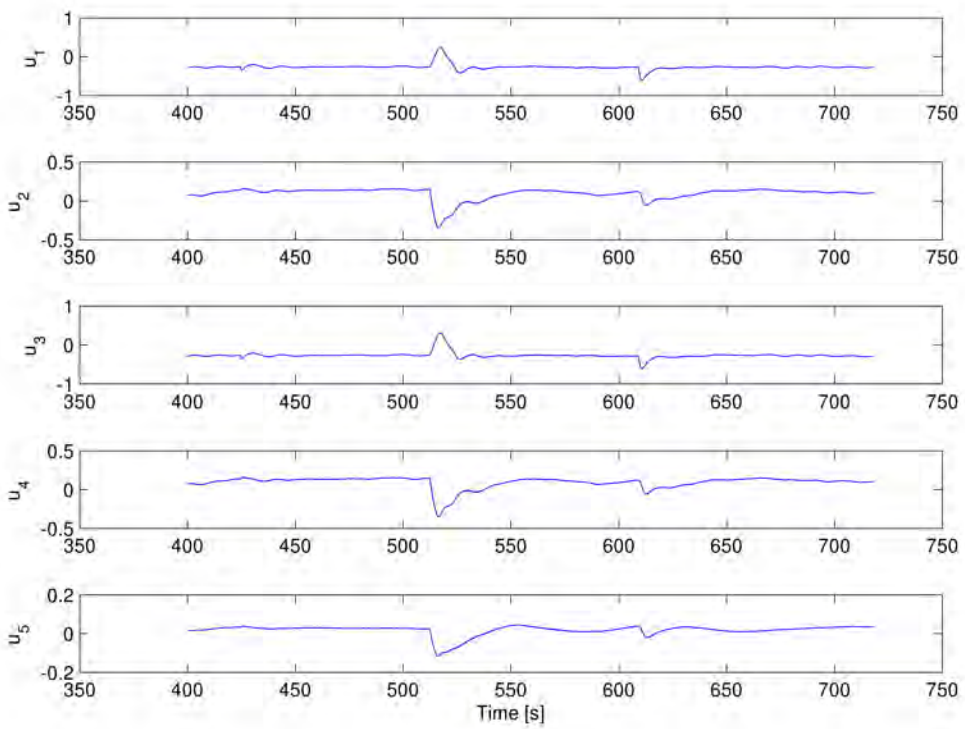

Figure 9.3: Thruster control signals from DP test

In Figure 9.3 one can see that the thrusters are to some extent oscillating. This is caused by the WF motion of the vessel, and should be removed by a decent wave filter. In Figure 9.1 on page 75 and Figure 9.2 on the preceding page it is observed that especially the heading is a bit off its desired heading. This might relate to the quick fix for the thruster allocation, where the bow thruster was tuned down. Another observation done when the vessel was in DP mode is that the bow thruster had some dead-band. The sound from the bow thruster is easy to distinguish when it is operating, even at low speeds. It sometimes happened that the DP system commanded small thrust commands for the bow thruster, and still the bow thruster did not operate. This might have been due to the inbuilt dead-band in the ESC for the bow thruster. Therefore, the heading error needed to be sufficiently large before the bow thruster started to operate, or the heading error needed to be present for some time such that the integrator in the controller could build up, and hence activate the bow thruster. Both these cases were experienced during testing of the DP system.

Part III

Discussion

Chapter 10

Discussion and recommendations

The first part of this work started out with the building of CSE1. Several major upgrades were conducted with respect to thrusters and instrumentation, to make it a good test platform for marine control engineering purposes, and for demonstrations. The platform is flexible in the sense that different I/O modules can easily be changed to meet new interface demands from new types of equipment. With respect to the software this new platform is a lot more flexible and easy to use than its predecessors in the MC Lab. LabView is relatively easy to work with, and premade functions exist to rapidly create advanced GUIs. Many of the subsequent users are believed to prefer Matlab/Simulink over LabView, but they can still use Simulink to make for instance controllers because of the SIT ad on in LabView.

During the testing of the manual control, where the PS3 controller was used to control the thrusters, it was found out that the PS3 controller was an excellent choice. There are several reasons for this. First of all the controller is wireless with a range of almost the entire basin. This allowed the user to operate the model ship from almost everywhere inside the basin/laboratory without having to deal with cables. The reliability of this controller was also impressive, meaning the controller's capacity to deliver precise input. Both the joysticks found on the PS3 controller are very accurate (16-bit), and the wireless connection and the drivers and software used proved very stable. Also, the cost of this controller is relatively low. All these factors combined implies that this controller can easily be utilized on other control applications were a cheap, wireless, and accurate input device is needed.

Expectations on how the model VSPs would perform on the model ship was high. The power of these propellers was maybe a bit out of proportion to the vessel at full speed, but in total this is better than having underpowered actuators. The ability to rapidly change thrust direction of the model VSPs was impressive. This is mostly related to the power and speeds of the servos that regulate the control rod position of the VSPs. The layout and configuration of these servos proved to work well. The method of using

lookup tables to calculate the PWM control signal worked very well. The new bow thruster functioned satisfactory as well, but also this was maybe a bit out of power proportions.

The upgrades done on CSE1 have really served its purpose for this work. However, there are two more things that should be improved for the vessel. The first is to have a proper "dead man's control", that cuts the power on the vessel. This is important to have if, for instance, the DP controller fails for some reason, if the wireless communication between the vessel and "land" gets interrupted. The Compact RIO aboard CSE1 is placed inside a waterproof box, but the ESCs and motors are still exposed to the open. The second recommended upgrade would be to design a deck, such that none of the equipment would be damaged in case of a water entry, or in the worst case a capsizing.

The process of system identification did not turn out the way one hoped. The surge and sway damping were established with proven methods, and the parameters obtained are believed to be reasonably accurate. When the thrust from the VSPs was mapped at 40% rotational speed, the speed versus pitch curves did not match well with any of the suggested thruster models. More effort should be focused on establish better models for these type of thruster, or for a DP application some sort of lookup table should be implemented to calculate the commanded pitch. The thrust from the VSPs was not symmetric. This indicates that the thruster-thruster and thruster-hull interaction is relatively large for this vessel. To account for this, even more sophisticated models of the entire thruster system are needed. During the parameter identification with the SITB, several weaknesses with this method were found. For instance that the estimated parameters where largely influenced by the constrains put on the parameters, that the numerical values of the estimated parameters would largely depend on the length of the analyzed data-series, and that under some conditions the entire analysis would not provide results at all. However, it is believed that the main reason that this method did not provide reliable results is that the simplified DP model used is not detailed enough to describe the data used during the analysis. A more sophisticated model that includes for instance nonlinear damping and accounts for the Coriolis effect should be used in this analysis to investigate if this improves the reliability of the results obtained.

When the joystick mode was tested on CSE1 for the first time, it had some issues related to high yaw rotation when sway was commanded. This is believed to be related to the thrust characteristics of the VSPs discussed in the previous paragraph. The thrust allocation was implemented with a linear model of the VSPs, and this simplification was not a reasonable assumption. The thrust allocation was adjusted by amplifying the force coefficient of the bow thruster in order to make it work. This fix provided a much better allocation, but the problem was most likely not caused by the force coefficient for the bow thruster being underestimated, but rather an overestimation of the force coefficient for the VSPs in the first place.

When the DP system was tested, it performed adequate after some tuning. It was in

advance believed to need some tuning, as the gain matrices for the controller was not based on the actual parameters of the vessel. The performance of the DP system could have been better with more tuning. The gains in the DP controller should be adjusted once a new and reliable system identification is in place. During the DP testing, it became clear that a wave filter of some sort was needed to reduce the oscillations on the thrusters, and hence reduce the wear and tear. While testing in the laboratory, this was not prioritized, and hence the wave filter is absent. The Qualisys system was able to provide accurate position and orientation measurements of CSE1, but in some cases it was observed that the system was unable to provide data, because the IR markers were shadowing each other. If the position and orientation estimates are lost for a longer period of time, it might result in the DP controller rendering the vessel out of control. Therefore, a dead reckoning system should be implemented. This can be obtained with for instance a Kalman filter. Another way to reduce the risk of loosing position and orientation estimates is to adjust the placement of the IR reflecting markers. The markers could be placed with larger height intervals, and hence reduce the risk of the reflectors shadowing each other. A new placement of the IR reflectors should be considered before conducting new experiments with the vessel, depending on the application.

The GUI that was built up in LabView provided an excellent way to control and monitor the vessel, for all operational modes. For all GUIs it is always a struggle between design and a functionality. One wants to present information to the user in a visually pleasant way, and have easy-to-use controls, this might however compromise the available functionality of the GUI. A 3D visualization of the model ship and the HIL model was implemented in the GUI. This provided an excellent way to easily run real-time testing to compare the real vessel and the HIL model. LabView has the ability to visualize 3D models in real time that Matlab/Simulink can not offer. These visualizations can relatively easily be created without for instance having to know a 3D programming language like OpenGL. The ability to visualize something in 3D is very nice for demonstration purposes, as this is something everyone can relate to without having a technical background. Mr. Wahl also indicated that the created 3D visualization models and setup might be used later by MARINTEK for other similar purposes. The 3D visualization has also gained a lot of attention from people passing by the MC Lab.

Chapter 11

Conclusions

Throughout the work with this thesis a new testing platform has been built up around the model ship CSE1. The vessel should be well suited for its purpose, that is, demonstrations and student experiments. However, some minor upgrades still remains, such as a "dead man's control" and a waterproof deck. The manual control of the vessel is working well, and the vessel is easy to control, much due to the PS3 controller.

The system identification only partially succeeded. Of the hydrodynamical coefficients, the surge and sway damping coefficients were established using towing tests, and are believed to be valid. Those parameters estimated with the SITB were not reliable. This is most likely because the grey-box model used for identification did not provide high enough fidelity for its application.

A working DP system was demonstrated, but the systems performance was not as great as hoped for. The performance could have been better if more time for tuning had been allocated, and a better thruster model for the VSPs had been used. The HIL model that was created provided a great way to test signal routing and scaling, but the implemented HIL model is not accurate enough to use for a complete substitute for the vessel. The GUI created for the vessel presents information to the user in a respectable way, and provides easy to use controls. The 3D visualization provides a great way to monitor the vessel, and a feature like this is well suited for demonstration purposes.

Bibliography

David Bray. *Dynamic Positioning*. Oilfield Publications Limited, 2003.

Cornwall Model Boats. Voith schneider and schottel drive units from cornwall model boats. `http://www.cornwallmodelboats.co.uk/acatalog/voith_schottel.html`, November 2010.

Odd Magnus Faltinsen. *Sea Loads on Ships and Offshore Structures*. The press syndicate of the university of Cambridge, The Pitt building, Trumpington Street, Cambridge CB2 1RP, United Kingdom, 1990.

Odd Magnus Faltinsen. *Hydrodynamics of high-speed marine vehicles*. The press syndicate of the university of Cambridge, 2005.

Thor Inge Fossen. *Guidance and Control of Marine Craft*. Norwegian University of Science and Technology, Trondheim, Norway, 2010.

Thor Inge Fossen, S.I. Sagatun, and Asgeir J. Sørensen. Identification of dynamically positioned ships. *Control Eng. Practice*, 4(3):369–376, 1996.

Graupner. Information on a product - graupner compact 460z. `http://shop.graupner.de/webuerp/servlet/AI?ARTN=7749`, May 2011.

International Maritime Organization. Guidlines for vessels with dynamic positioning systems. *MSC/Circ.645*, 1994.

Birgit Jürgens and Werner Fork. *The Facination of the Voith-Schneider Propeller - History and Engineering*. Koehlers Verlagsgesellschaft mbH, Hamburg, 2002.

Dirk Jürgens and Michael Palm. Voith schneider propeller - an efficient propulsion system for dp controlled vessels.

komplett.no. Sony wireless dual shock controller. `http://www.komplett.no/k/ki.aspx?sku=366170`.

Kongsberg Maritime. Dynamic positioning - basic principles. `http://www.km.kongsberg.com/ks/web/nokbg0240.nsf/AllWeb/BD306BBB3E7DA73FC1256DAB00353083?OpenDocument`, May 2011.

Edward M. Lewandowski. *The dynamics of marine craft: maneuvering and seakeeping*. World Scientific Publishing Co. Pte. Ltd, 2004.

Davies Lim. Use ps3 controller in windows 7, vista and xp (wireless bluetooth). `http://www.davieslim.com/ps3/use-ps3-controller-in-windows-wireless-bluetooth/`, May 2011.

Voith Turbo Marine. Offshore supply vessels - summary of development and model testing. Technical report, 2005.

J.Michael McCarthy and Gim Song Soh. *Geometric Design of Linkages*. Springer, Springer New York Dordecht Heidelberg London, 2010.

Model Slipway. Anchor handling tug aziz / arif. `http://www.modelslipway.com/aziz.htm`, April 2011.

National Instruments. Pulse width modulation (pwm) using ni-daqmx and labview. `http://zone.ni.com/devzone/cda/tut/p/id/2991`, May 2011.

Norwegian University of Science and Technology. Marine cybernetics laboratory. `http://www.ntnu.no/imt/lab/kybernetikk`, November 2010.

Ben R. Rich. Clarence leonard (kelly) johnson - biographical memoirs. `http://www.nap.edu/readingroom.php?book=biomems&page=cjohnson.html`, 2011.

Hugo Ryvik. Århundrets norske ingeniørbragd. `http://web.tu.no/nyheter/arkiv/?id=1999/33/s2425/s2425.html`, May 2011.

Roger Skjetne. *The Maneuvering Problem*. PhD thesis, NTNU, 2005.

Roger Skjetne and Olav Egeland. Hardware-in-the-loop testing of marine control systems. *Modeling, Identification and Control*, 27(4):239–258, 2006.

Roger Skjetne, Øyvind N. Smogeli, and Thor Inge Fossen. A nonlinear ship manoeuvering model: Identification and adaptive control with experiments for a model ship. *Modeling, Identification and Control*, 25(1):3–27, 2004.

SNAME. Nomenclature for treating the motion of a submerged body through a fluid. Technical report, April 1950. Technical and Reserach Bulletin No. 1-5.

Asgeir J. Sørensen. *Marine Cybernetics - Modelling and Control*. Norwegian University of Science and Technology, Trondheim, Norway, 2005.

Voith Turbo. Voith turbo - voith schneider propeller. `http://www.voithturbo.de/vt_en_pua_marine_vspropeller.htm`, December 2010.

Østensjø Rederi. Edda fram general description. `http://www.ostensjo.no/ostensjo/web.nsf/Pages/EddaFram`, December 2010a.

Østensjø Rederi. Edda accommodation. `http://www.eddaaccommodation.com/`, December 2010b.

Appendix A

CD content

All the appendixes are found digitally on the attached CD-ROM. The CD contains the following;

- PDF document
- Matlab code
- LabView program
- A video of CS Enterprise 1